

## THE Fe XIV SPECTRUM: PREDICTED LINE INTENSITIES AND SOLAR IDENTIFICATIONS

A. K. BHATIA

Astronomy Branch, Laboratory for Astronomy and Solar Physics, Goddard Space Flight Center, Greenbelt, MD 20771

S. O. KASTNER

Mathematical Science Consultants, Inc., 1-A Ridge Road, Greenbelt, MD 20770

F. P. KEENAN AND E. S. CONLON

Department of Pure and Applied Physics, The Queen's University of Belfast, Belfast BT7 1NN, Northern Ireland

AND

K. G. WIDING

E. O. Hulbert Center for Space Research, Code 4174W, US Naval Research Laboratory, Washington, DC 20375-5000

Received 1993 July 19; accepted 1993 November 19

### ABSTRACT

Level populations and line intensities have been calculated in a 40-level model of Fe XIV which includes the configurations  $3p^3$  and  $3s3p3d$ . The results have been compared against intensities of weaker, unidentified, or tentatively classified lines in published solar line lists including a recent GSFC/SERTS high-resolution list, and in presently measured archival NRL/S082A active region spectra. Seven new lines are identified as Fe XIV transitions; five other observed, unidentified lines are considered to be Fe XIV transitions on the basis of wavelength coincidence, but require further observations to obtain photometric intensities for verification; one line at 216.93 Å is shown to be due to some other ion than Fe XIV. In addition, a unique forbidden infrared ( $\approx 1.25 \mu\text{m}$ ) line originating in the high metastable level  $3s3p3d(^4F_{9/2})$  is found to have an unusual intensity dependence on electron density.

*Subject headings:* atomic data — line: identification — Sun: corona — Sun: general — Sun: UV radiation

### 1. INTRODUCTION

The Fe XIV spectrum has been of continuing interest for both theoretical and observational reasons. The ground configuration is  $3s^23p$  outside a closed-shell core so that three-electron configurations such as  $3s3p^2$ ,  $3p^3$ , and  $3s3p3d$  can be excited which involve doublet and quartet terms. A total of four odd configurations and five even configurations are present in the ground  $n = 3$  complex. The stronger resonance line multiplets between doublet terms are prominent in the solar spectrum and were first discussed quantitatively by Blaha (1971)(MB). The quartet system and intercombination lines have however come under study only recently. Trabert, Hutton, & Martinson (1987) identified the  $3s^23p(^2P)-3s3p(^2P)$  intercombination lines in beam-foil spectra and in the solar flare spectrum of Dere (1978). A comprehensive laboratory investigation was carried out by Redfors & Litzen (1989)(RL) which has improved knowledge of the  $3p^3$  and  $3s3p3d$  levels in elements from calcium up to nickel. On the basis of the RL wavelengths Kastner (1991)(SK) has proposed identifications of some weaker solar lines.

On the theoretical side, multiconfiguration calculations of transition rates in Fe XIV have been carried out by Farrag, Luc-Koenig, & Sinzelle (1982), Fawcett (1983), Froese Fischer and Liu (1986)(FL), and Huang (1986)(KH). More recently Dufton and Kingston (1991)(DK) have used  $R$ -matrix close-coupled calculations to produce effective collision strengths between the 12 levels of the three lower configurations  $3s^23p$ ,  $3s3p^2$ , and  $3s^23d$ . Keenan et al. (1991a) made use of the DK and FL data to derive electron densities from the solar Fe XIV resonance lines, which were found to be in good agreement with densities obtained from lines of Fe XII and Fe XIII. The same workers (Keenan et al. 1991b) verified the solar intercombination line identifications of Trabert et al. and found

them in flare spectra registered by the NRL S082A slitless spectrograph flown on *Skylab* (Dere et al. 1979).

The weaker solar lines proposed by SK to be Fe XIV transitions would originate in levels of the higher  $3p^3$  and  $3s3p3d$  configurations. To check the proposed identifications it is therefore necessary to include these configurations in a calculation of expected line intensities. This has been done in the present work which gives the level populations and relative line intensities resulting from a five-configuration, 40-level model of Fe XIV, and compares the predictions with several sets of solar observations including new S082A spectral data.

Other items of related interest are discussed below, including an unusual forbidden line expected from a high quartet level.

### 2. CALCULATION AND RESULTS

The present Fe XIV model includes the five configurations  $3s^23p$ ,  $3s3p^2$ ,  $3s^23d$ ,  $3p^3$ , and  $3s3p3d$  giving 40 doublet and quartet levels. Allowed and forbidden radiative transition rates between these levels were obtained using the SUPERSTRUCTURE program (Eissner, Jones, & Nussbaumer 1972). To obtain collisional excitation rates, the program package of Eissner & Seaton (1972) was used to calculate reactance matrices in the distorted wave approximation and collision strengths between the fine structure levels were obtained using the JJOM program of Saraph (1972), at three incident energies above the highest threshold of about 8 rydbergs. The resulting atomic data are tabulated in a separate publication (Bhatia & Kastner 1993). The presently calculated transition rates are there compared with those of KH and FL and found to be in reasonable agreement. A comparison of our calculated collision strengths with those in Table 2 of DK also shows quite good agreement. For optimum accuracy in the present computation of level populations and line intensities, however, we

used the effective collision strengths of DK where available, i.e., between levels of the lower three configurations.

Fe xv level populations and line intensities were computed over the electron density range  $\log N_e$  ( $\text{cm}^{-3}$ ) = 8.0 (0.5) 12.0 and the electron temperature range  $\log T_e$  = 6.0 (0.2) 6.4, the intermediate temperature of  $\log T_e$  = 6.2 ( $T_e = 1.58 \times 10^6 \text{ K}$ ) corresponding to the approximate temperature of maximum Fe xiv ion abundance in an optically thin plasma (Arnaud & Rothenflug 1985). The strong resonance line at 211.33 Å (transition 11 → 1; notation keyed to Table 1) was chosen as reference line. This is not necessarily the best choice for a reference line when optical depth effects are nonnegligible, since a forbidden line is then more suitable if available (cf. Bhatia & Kastner 1989). However, the given line intensities may be converted straightforwardly into line intensities (in energy units) relative to one of the intercombination lines of the  $3s^2 3p(^2P)$ – $3s3p(^4P)$  multiplet, or one of the stronger subordinate lines, if such lines are present in the spectrum being investigated.

The numerical results of the calculation are presented in Tables 1 to 8. Table 1 lists the levels and calculated energies together with the laboratory-observed energies according to

TABLE 1  
Fe XIV ENERGY LEVELS<sup>a</sup>

INDEX	CONFIGURATION	LEVEL	ENERGY (cm <sup>-1</sup> )	
			Calculated	Observed <sup>b</sup>
1.....	$3s^2 3p$	$^2P_{1/2}$	0	0
2.....	...	$^2P_{3/2}$	17327	18853
3.....	$3s3p^2$	$^4P_{1/2}$	226839	225095
4.....	...	$^4P_{3/2}$	233811	232805
5.....	...	$^4P_{5/2}$	243001	242401
6.....	...	$^2D_{3/2}$	310864	299247
7.....	...	$^2D_{5/2}$	312464	301474
8.....	...	$^2S_{1/2}$	383970	364697
9.....	...	$^2P_{1/2}$	418685	388529
10.....	...	$^2P_{3/2}$	428167	396525
11.....	$3s^2 3d$	$^2D_{3/2}$	499570	473216
12.....	...	$^2D_{5/2}$	502147	475190
13.....	$3p^3$	$^2D_{3/2}$	578198	576388
14.....	...	$^2D_{5/2}$	581187	580273
15.....	...	$^4S_{3/2}$	597467	589005
16.....	$3s3p3d$	$^4F_{3/2}$	642806	
17.....	...	$^4F_{5/2}$	646672	
18.....	...	$^4F_{7/2}$	652299	
19.....	$3p^3$	$^2P_{1/2}$	654608	642310
20.....	...	$^2P_{3/2}$	656413	645416
21.....	$3s3p3d$	$^4F_{9/2}$	660034	
22.....	...	$^4P_{5/2}$	694685	690308
23.....	...	$^4D_{3/2}$	696803	692590
24.....	...	$^4D_{1/2}$	698474	694191
25.....	...	$^4P_{1/2}$	705747	
26.....	...	$^4P_{3/2}$	706934	
27.....	...	$^4D_{5/2}$	707812	704147
28.....	...	$^4D_{7/2}$	707957	703383
29.....	...	$^2D_{3/2}$	733459	717253
30.....	...	$^2D_{5/2}$	733622	717865
31.....	...	$^2F_{5/2}$	758396	744971
32.....	...	$^2F_{7/2}$	772179	759834
33.....	...	$^2P_{3/2}$	829567	807097
34.....	...	$^2P_{1/2}$	830057	
35.....	...	$^2F'_{7/2}$	843202	817614
36.....	...	$^2F'_{5/2}$	845694	820583
37.....	...	$^2D'_{3/2}$	872034	840767
38.....	...	$^2D'_{5/2}$	876082	844512
39.....	...	$^2P'_{1/2}$	876809	839491
40.....	...	$^2P'_{3/2}$	880198	843689

<sup>a</sup> Primed terms of the  $3s3p3d$  configuration have  $^1P$  parentage.

<sup>b</sup> Redfors & Litzen 1989.

TABLE 2A  
Fe XIV LINES<sup>a,b</sup>

Levels <sup>c</sup> <i>i-j</i>	Line	$\lambda$ (Å)	Levels <sup>c</sup> <i>i-j</i>	Line	$\lambda$ (Å)
1–2.....	<i>M</i>	5302.86	19.....	<i>x</i>	291.49
3.....	<i>N</i>	444.25	20.....	<i>y</i>	(288.88)
4.....	<i>O</i>	429.54	29.....	<i>z</i>	(239.23)
6.....	<i>B</i>	334.17	30.....	<i>aa</i>	(238.88)
8.....	<i>I</i>	274.20	31.....	<i>ab</i>	224.35
9.....	<i>F</i>	257.38	36.....	<i>ac</i>	(191.81)
10.....	<i>G</i>	252.19	7–13.....	<i>ad</i>	(363.75)
11.....	<i>J</i>	211.33	14.....	<i>ae</i>	358.68
2–3.....	<i>P</i>	484.60	17.....	<i>af</i>	<sup>e</sup>
4.....	<i>Q</i>	467.40	20.....	<i>ag</i>	290.75
5.....	<i>R</i>	447.36	29.....	<i>ah</i>	(240.51)
6.....	<i>C</i>	356.64 <sup>d</sup>	30.....	<i>ai</i>	240.16
7.....	<i>A</i>	353.83	7–31.....	<i>aj</i>	(225.48)
8.....	<i>H</i>	289.12	32.....	<i>ak</i>	218.17
9.....	<i>D</i>	270.51	33.....	<i>al</i>	(197.78)
10.....	<i>E</i>	264.79	35.....	<i>am</i>	(193.75)
11.....	<i>L</i>	220.08	8–20.....	<i>an</i>	(356.23)
12.....	<i>K</i>	219.14	33.....	<i>ao</i>	226.04
3–23.....	<i>b</i>	213.91	34.....	<i>ap</i>	<sup>e</sup>
24.....	<i>c</i>	213.18	9–13.....	<i>aq</i>	(532.31)
4–16.....	<i>e</i>	<sup>e</sup>	37.....	<i>at</i>	(221.12)
17.....	<i>f</i>	<sup>e</sup>	39.....	<i>au</i>	(221.75)
20.....	<i>g</i>	(242.36)	10–14.....	<i>av</i>	(544.22)
22.....	<i>h</i>	218.58	20.....	<i>aw</i>	(401.78)
25.....	<i>i</i>	<sup>e</sup>	33.....	<i>ax</i>	(243.56)
26.....	<i>j</i>	<sup>e</sup>	38.....	<i>az</i>	223.22
27.....	<i>k</i>	212.15	39.....	<i>ba</i>	(225.75)
5–13.....	<i>l</i>	(299.41)	40.....	<i>bb</i>	223.62
14.....	<i>m</i>	(295.97)	11–31.....	<i>bc</i>	(367.99)
15.....	<i>n</i>	288.51	36.....	<i>bd</i>	287.86
17.....	<i>o</i>	<sup>e</sup>	37.....	<i>be</i>	269.93
18.....	<i>p</i>	<sup>e</sup>	39.....	<i>bf</i>	273.00
22.....	<i>pp</i>	223.26	40.....	<i>bg</i>	(269.93)
26.....	<i>q</i>	<sup>e</sup>	12–31.....	<i>bh</i>	(370.67)
27.....	<i>r</i>	216.58	32.....	<i>bi</i>	(351.32)
28.....	<i>s</i>	216.93	35.....	<i>bj</i>	292.04
32.....	<i>t</i>	(193.26)	37.....	<i>bk</i>	273.54
6–13.....	<i>u</i>	(360.83)	38.....	<i>bl</i>	270.77
14.....	<i>v</i>	(355.84)	40.....	<i>bm</i>	(271.37)
16.....	<i>w</i>	<sup>e</sup>	18–21.....	<i>bn</i>	(12500.)

<sup>a</sup> Redfors & Litzen 1989; Shirai et al. 1990; Levashov et al. 1990.

<sup>b</sup> Wavelengths in parentheses unobserved; from known levels.

<sup>c</sup> Keyed to Table 1.

<sup>d</sup> Observed by SERTS (Thomas & Neupert 1993).

<sup>e</sup> Wavelengths associated with unknown levels.

RL (these differ somewhat from the solar-derived values of Behring et al. (1976)(BCFD) as may be seen in Table 2 of SK which compares wavelengths). Table 2A lists the Fe xiv transitions found to be of intensity greater than about one-thousandth the intensity of the reference line. Resonance lines and intercombination lines associated with the two ground levels are denoted by capital letters (consistent with designations in an earlier publication on the aluminum-like spectra; Kastner 1985), while all other lines are denoted by lower-case letters. The wavelengths fall into three classes: (a) observed laboratory wavelengths taken from RL; (b) wavelengths given in parentheses for previously unobserved lines, calculated from the known levels; and (c) wavelengths not given (footnote e), for transitions associated with the unknown levels 16, 17, 18, 34.

The important visible forbidden line at 5302.86 Å is included. The intensity of this line was earlier treated quantitatively by Petrini (1970) and Mason (1975). However the

TABLE 2B  
COMPARISON OF Fe XIV LINE  
DESIGNATIONS

TRANSITION <sup>a</sup>		LINE DESIGNATION	
<i>j</i> → <i>i</i>		<i>MB</i> <sup>b</sup>	Present
11	1.....	1	<i>J</i>
8	1.....	2	<i>I</i>
10	2.....	3	<i>E</i>
6	1.....	4	<i>B</i>
11	2.....	5	<i>L</i>
9	2.....	6	<i>D</i>
9	1.....	7	<i>F</i>
10	1.....	8	<i>G</i>
31	6.....	9	<i>ab</i>
12	2.....	10	<i>K</i>
7	2.....	13	<i>A</i>
8	2.....	14	<i>H</i>
37	9.....	16	<i>at</i>
31	7.....	17	<i>aj</i>
38	10.....	18	<i>az</i>
33	7.....	21	<i>al</i>
32	7.....	25	<i>ak</i>

<sup>a</sup> Keyed to Table 1.<sup>b</sup> Blaha 1971.

TABLE 3A  
RELATIVE LEVEL POPULATIONS;  $\log T_e = 6.0$

LEVEL <sup>a</sup>	log $N_e$				
	8.0	8.5	9.0	9.5	10.0
1.....	0.985+0	0.954+0	0.874+0	0.720+0	0.543+0
2.....	0.152-1	0.458-1	0.126+0	0.279+0	0.453+0
3.....	0.224-9	0.694-9	0.208-8	0.583-8	0.158-7
4.....	0.195-8	0.610-8	0.187-7	0.560-7	0.167-6
5.....	0.461-9	0.150-8	0.511-8	0.182-7	0.643-7
6.....	0.720-10	0.222-9	0.653-9	0.176-8	0.449-8
7.....	0.169-10	0.598-10	0.243-9	0.109-8	0.464-8
8.....	0.794-11	0.247-10	0.747-10	0.216-9	0.607-9
9.....	0.702-11	0.218-10	0.653-10	0.185-9	0.505-9
10.....	0.388-11	0.128-10	0.452-10	0.171-9	0.640-9
11.....	0.810-11	0.249-10	0.731-10	0.197-9	0.496-9
12.....	0.350-12	0.188-11	0.123-10	0.774-10	0.384-9
13.....	0.384-11	0.119-10	0.354-10	0.986-10	0.263-9
14.....	0.257-11	0.826-11	0.273-10	0.931-10	0.319-9
15.....	0.507-15	0.222-14	0.122-13	0.696-13	0.333-12
16.....	0.679-11	0.208-10	0.611-10	0.163-9	0.408-9
17.....	0.758-11	0.234-10	0.696-10	0.193-9	0.515-9
18.....	0.714-11	0.234-10	0.805-10	0.282-9	0.913-9
19.....	0.348-14	0.295-13	0.246-12	0.171-11	0.875-11
20.....	0.240-12	0.763-12	0.245-11	0.798-11	0.260-10
21.....	0.417-5	0.326-4	0.245-3	0.133-2	0.410-2
22.....	0.646-13	0.199-12	0.584-12	0.160-11	0.435-11
23.....	0.287-13	0.886-13	0.263-12	0.723-12	0.190-11
24.....	0.106-13	0.329-13	0.987-13	0.278-12	0.758-12
25.....	0.593-15	0.304-14	0.194-13	0.121-12	0.611-12
26.....	0.168-14	0.720-14	0.386-13	0.220-12	0.106-11
27.....	0.481-14	0.174-13	0.732-13	0.347-12	0.155-11
28.....	0.139-13	0.454-13	0.156-12	0.570-12	0.210-11
29.....	0.618-13	0.191-12	0.574-12	0.162-11	0.442-11
30.....	0.802-13	0.250-12	0.763-12	0.224-11	0.651-11
31.....	0.144-11	0.445-11	0.131-10	0.354-10	0.905-10
32.....	0.188-13	0.176-12	0.152-11	0.107-10	0.550-10
33.....	0.156-12	0.481-12	0.144-11	0.400-11	0.107-10
34.....	0.226-14	0.131-13	0.912-13	0.590-12	0.296-11
35.....	0.169-13	0.533-13	0.167-12	0.521-12	0.162-11
36.....	0.567-14	0.188-13	0.670-13	0.257-12	0.975-12
37.....	0.515-13	0.160-12	0.485-12	0.140-11	0.397-11
38.....	0.312-13	0.103-12	0.360-12	0.135-11	0.503-11
39.....	0.149-14	0.601-14	0.299-13	0.160-12	0.744-12
40.....	0.617-14	0.217-13	0.866-13	0.383-12	0.160-11

TABLE 3B  
RELATIVE LEVEL POPULATIONS;  $\log T_e = 6.0$

LEVEL <sup>a</sup>	log $N_e$			
	10.5	11.0	11.5	12.0
1.....	0.429+0	0.380+0	0.362+0	0.357+0
2.....	0.564+0	0.612+0	0.628+0	0.633+0
3.....	0.445-7	0.134-6	0.414-6	0.130-5
4.....	0.510-6	0.159-5	0.501-5	0.158-4
5.....	0.214-6	0.689-6	0.219-5	0.695-5
6.....	0.120-7	0.348-7	0.107-6	0.334-6
7.....	0.170-7	0.570-7	0.184-6	0.585-6
8.....	0.176-8	0.537-8	0.167-7	0.527-7
9.....	0.143-8	0.431-8	0.134-7	0.421-7
10.....	0.222-8	0.730-8	0.234-7	0.743-7
11.....	0.131-8	0.380-8	0.116-7	0.363-7
12.....	0.149-8	0.510-8	0.165-7	0.527-7
13.....	0.733-9	0.219-8	0.676-8	0.212-7
14.....	0.106-8	0.341-8	0.108-7	0.344-7
15.....	0.128-11	0.436-11	0.142-10	0.466-10
16.....	0.107-8	0.308-8	0.940-8	0.294-7
17.....	0.144-8	0.430-8	0.133-7	0.419-7
18.....	0.272-8	0.816-8	0.252-7	0.790-7
19.....	0.344-10	0.118-9	0.383-9	0.122-8
20.....	0.839-10	0.268-9	0.848-9	0.268-8
21.....	0.714-2	0.886-2	0.953-2	0.976-2
22.....	0.128-10	0.395-10	0.124-9	0.394-9
23.....	0.523-11	0.155-10	0.478-10	0.150-9
24.....	0.215-11	0.647-11	0.201-10	0.633-10
25.....	0.241-11	0.829-11	0.270-10	0.866-10
26.....	0.415-11	0.142-10	0.462-10	0.148-9
27.....	0.591-11	0.202-10	0.655-10	0.210-9
28.....	0.731-11	0.241-10	0.773-10	0.246-9
29.....	0.125-10	0.378-10	0.117-9	0.369-9
30.....	0.194-10	0.599-10	0.188-9	0.592-9
31.....	0.242-9	0.705-9	0.216-8	0.677-8
32.....	0.216-9	0.742-9	0.241-8	0.769-8
33.....	0.298-10	0.889-10	0.275-9	0.864-9
34.....	0.116-10	0.396-10	0.128-9	0.410-9
35.....	0.507-11	0.160-10	0.505-10	0.160-9
36.....	0.341-11	0.112-10	0.360-10	0.114-9
37.....	0.116-10	0.353-10	0.110-9	0.347-9
38.....	0.174-10	0.571-10	0.183-9	0.581-9
39.....	0.283-11	0.959-11	0.310-10	0.988-10
40.....	0.586-11	0.196-10	0.631-10	0.201-9

<sup>a</sup> Keyed to Table 1.

present work relates its intensity to those of the EUV lines, a useful feature for solar work (e.g., Neupert 1986). One other unique forbidden line of interest mentioned in the Introduction is also included in the list as line bn, between the close levels  $^4F_{9/2}$  and  $^4F_{7/2}$  of the  $3s3p3d$  configuration.

Because of the uncertain energies of the higher Fe XIV levels their numerical designations by previous authors have differed. For convenience Table 2B correlates the line designations of MB with the present letter designations (see also Table 1 of Kastner 1985 which correlates the present level designations with the more general designations of Farrag et al. 1982).

The relative populations of the 40 levels are tabulated in Tables 3, 4, and 5 for temperatures of  $\log T_e = 6.0, 6.2$ , and  $6.4$ , over the range of densities  $\log N_e = 8.0, 8.5, \dots, 12.0$ . Tables 6, 7, and 8 give the relative intensities of the lines listed in Table 2A, over the same ranges of density and temperature.

We stress that the numerical results given in Tables 3–8 correspond to the optically thin case. In future work it is expected that the calculations will be extended to obtain Fe XIV level populations and line intensities under optically thick conditions, which may be present, for example, in the solar situation.

TABLE 4A  
RELATIVE LEVEL POPULATIONS;  $\log T_e = 6.2$

LEVEL <sup>a</sup>	log $N_e$				
	8.0	8.5	9.0	9.5	10.0
1.....	0.985+0	0.956+0	0.879+0	0.728+0	0.549+0
2.....	0.145-1	0.438-1	0.121+0	0.271+0	0.446+0
3.....	0.212-9	0.655-9	0.196-8	0.551-8	0.148-7
4.....	0.174-8	0.545-8	0.167-7	0.501-7	0.149-6
5.....	0.429-9	0.140-8	0.475-8	0.169-7	0.598-7
6.....	0.782-10	0.241-9	0.709-9	0.192-8	0.485-8
7.....	0.173-10	0.614-10	0.250-9	0.113-8	0.484-8
8.....	0.974-11	0.302-10	0.906-10	0.256-9	0.696-9
9.....	0.709-11	0.220-10	0.665-10	0.190-9	0.527-9
10.....	0.423-11	0.140-10	0.489-10	0.184-9	0.688-9
11.....	0.914-11	0.281-10	0.829-10	0.224-9	0.565-9
12.....	0.370-12	0.201-11	0.134-10	0.854-10	0.430-9
13.....	0.421-11	0.130-10	0.389-10	0.109-9	0.290-9
14.....	0.281-11	0.904-11	0.298-10	0.102-9	0.347-9
15.....	0.500-15	0.224-14	0.125-13	0.731-13	0.356-12
16.....	0.685-11	0.211-10	0.619-10	0.166-9	0.415-9
17.....	0.766-11	0.237-10	0.706-10	0.196-9	0.522-9
18.....	0.723-11	0.237-10	0.813-10	0.287-9	0.941-9
19.....	0.372-14	0.318-13	0.268-12	0.188-11	0.975-11
20.....	0.274-12	0.872-12	0.280-11	0.909-11	0.296-10
21.....	0.407-5	0.319-4	0.245-3	0.141-2	0.475-2
22.....	0.671-13	0.206-12	0.608-12	0.166-11	0.449-11
23.....	0.298-13	0.921-13	0.274-12	0.756-12	0.198-11
24.....	0.111-13	0.343-13	0.103-12	0.290-12	0.789-12
25.....	0.607-15	0.307-14	0.194-13	0.122-12	0.618-12
26.....	0.174-14	0.738-14	0.390-13	0.222-12	0.108-11
27.....	0.502-14	0.180-13	0.750-13	0.352-12	0.158-11
28.....	0.145-13	0.472-13	0.161-12	0.587-12	0.216-11
29.....	0.733-13	0.227-12	0.681-12	0.192-11	0.521-11
30.....	0.950-13	0.296-12	0.903-12	0.265-11	0.762-11
31.....	0.175-11	0.540-11	0.159-10	0.433-10	0.110-9
32.....	0.217-13	0.204-12	0.177-11	0.125-10	0.654-10
33.....	0.196-12	0.605-12	0.181-11	0.505-11	0.135-10
34.....	0.261-14	0.154-13	0.109-12	0.713-12	0.362-11
35.....	0.191-13	0.601-13	0.189-12	0.588-12	0.183-11
36.....	0.643-14	0.213-13	0.756-13	0.289-12	0.110-11
37.....	0.664-13	0.207-12	0.627-12	0.181-11	0.512-11
38.....	0.401-13	0.132-12	0.460-12	0.172-11	0.640-11
39.....	0.174-14	0.710-14	0.359-13	0.196-12	0.927-12
40.....	0.773-14	0.271-13	0.108-12	0.477-12	0.201-11

TABLE 4B  
RELATIVE LEVEL POPULATIONS;  $\log T_e = 6.2$

LEVEL <sup>a</sup>	log $N_e$			
	10.5	11.0	11.5	12.0
1.....	0.431+0	0.380+0	0.362+0	0.356+0
2.....	0.560+0	0.608+0	0.625+0	0.631+0
3.....	0.415-7	0.124-6	0.383-6	0.120-5
4.....	0.456-6	0.143-5	0.449-5	0.142-4
5.....	0.199-6	0.639-6	0.203-5	0.643-5
6.....	0.128-7	0.369-7	0.113-6	0.353-6
7.....	0.179-7	0.600-7	0.194-6	0.617-6
8.....	0.196-8	0.587-8	0.182-7	0.571-7
9.....	0.151-8	0.455-8	0.141-7	0.445-7
10.....	0.239-8	0.785-8	0.251-7	0.799-7
11.....	0.149-8	0.429-8	0.131-7	0.410-7
12.....	0.168-8	0.577-8	0.187-7	0.597-7
13.....	0.803-9	0.238-8	0.736-8	0.231-7
14.....	0.115-8	0.370-8	0.118-7	0.373-7
15.....	0.138-11	0.472-11	0.154-10	0.502-10
16.....	0.108-8	0.310-8	0.946-8	0.296-7
17.....	0.145-8	0.433-8	0.134-7	0.420-7
18.....	0.279-8	0.827-8	0.253-7	0.792-7
19.....	0.386-10	0.133-9	0.431-9	0.138-8
20.....	0.952-10	0.303-9	0.960-9	0.304-8
21.....	0.894-2	0.115-1	0.126-1	0.130-1
22.....	0.132-10	0.410-10	0.129-9	0.410-9
23.....	0.542-11	0.160-10	0.494-10	0.155-9
24.....	0.223-11	0.669-11	0.207-10	0.652-10
25.....	0.245-11	0.848-11	0.276-10	0.887-10
26.....	0.423-11	0.146-10	0.474-10	0.152-9
27.....	0.605-11	0.207-10	0.675-10	0.216-9
28.....	0.751-11	0.248-10	0.795-10	0.253-9
29.....	0.147-10	0.439-10	0.136-9	0.427-9
30.....	0.226-10	0.693-10	0.217-9	0.684-9
31.....	0.294-9	0.853-9	0.261-8	0.817-8
32.....	0.260-9	0.893-9	0.290-8	0.926-8
33.....	0.374-10	0.111-9	0.343-9	0.108-8
34.....	0.143-10	0.490-10	0.159-9	0.508-9
35.....	0.572-11	0.180-10	0.568-10	0.180-9
36.....	0.385-11	0.127-10	0.406-10	0.129-9
37.....	0.148-10	0.451-10	0.140-9	0.443-9
38.....	0.222-10	0.728-10	0.233-9	0.740-9
39.....	0.355-11	0.121-10	0.391-10	0.125-9
40.....	0.740-11	0.248-10	0.799-10	0.254-9

<sup>a</sup> Keyed to Table 1.

The predicted density variations of the resonance lines and intercombination lines are shown in Figure 1, for  $\log T_e = 6.2$ . A comparison with Figure 1 of MB shows that the latter figure is in quite good quantitative agreement with the new results for the most part. One exception is line C which was not included by MB. Also MB did not include the intercombination lines, originating in the  $3s3p^2(^4P)$  term, which have now been observed as mentioned above; as seen in Figure 1 the strongest intercombination line R can reach a relative intensity of about 1/30 compared to the strong reference line J.

The density variations of the stronger subordinate lines are plotted in Figure 2. Lines ab and ak were found to be fairly strong also by MB. We find here that line ak at 218.17 Å reaches an intensity of greater than 1/10 that of reference line J, at the higher densities. As mentioned above, a principal motivation for the present work was the question of whether some of these subordinate lines are present in solar spectra. From Figure 2 it is already seen that lines such as ab and ak are certainly to be expected.

Figure 3 shows the relatively small dependence of the lines on temperature (above  $T_e = 10^6$  K), whether allowed (C), inter-

combination (P), or forbidden (M, bn). More will be said below about the unusual density dependence of line bn.

### 3. COMPARISONS WITH OBSERVATIONS

These results allow us to draw quantitative conclusions on whether some of the weaker Fe XIV lines have been registered in the solar spectrum of BCFD (1976) as proposed by SK, as well as in other published solar spectra. We have also obtained observed ratios for some of the lines in the *Skylab* S082A spectra.

#### 3.1. Analysis of Published Spectra

There exist at least four relevant published spectra in the general range of interest. These are the photoelectric spectrum of Malinovsky & Heroux (1973) (MH) covering the range 50–300 Å, which recorded lines from a whole solar active disk; the photographic spectrum of Behring et al. (1976) (BCFD) which covers the range 164–765 Å, also recording a whole solar disk (with activity present as shown below); the photographic spectrum of Dere (1978) (D78) covering the range 171–630 Å, which combined lines from individual solar flares;

TABLE 5A  
RELATIVE LEVEL POPULATIONS;  $\log T_e = 6.4$

LEVEL <sup>a</sup>	$\log N_e$				
	8.0	8.5	9.0	9.5	10.0
1.....	0.987+0	0.960+0	0.888+0	0.742+0	0.562+0
2.....	0.133-1	0.403-1	0.112+0	0.257+0	0.433+0
3.....	0.186-9	0.578-9	0.174-8	0.489-8	0.131-7
4.....	0.146-8	0.455-8	0.140-7	0.420-7	0.125-6
5.....	0.371-9	0.121-8	0.409-8	0.146-7	0.518-7
6.....	0.771-10	0.238-9	0.703-9	0.191-8	0.481-8
7.....	0.160-10	0.566-10	0.230-9	0.105-8	0.455-8
8.....	0.105-10	0.326-10	0.975-10	0.273-9	0.726-9
9.....	0.663-11	0.207-10	0.628-10	0.182-9	0.511-9
10.....	0.422-11	0.138-10	0.482-10	0.180-9	0.675-9
11.....	0.932-11	0.288-10	0.852-10	0.232-9	0.587-9
12.....	0.345-12	0.189-11	0.127-10	0.829-10	0.428-9
13.....	0.405-11	0.126-10	0.377-10	0.106-9	0.282-9
14.....	0.271-11	0.869-11	0.285-10	0.967-10	0.331-9
15.....	0.449-15	0.200-14	0.112-13	0.666-13	0.331-12
16.....	0.635-11	0.196-10	0.578-10	0.156-9	0.391-9
17.....	0.711-11	0.220-10	0.659-10	0.184-9	0.489-9
18.....	0.670-11	0.219-10	0.749-10	0.266-9	0.886-9
19.....	0.340-14	0.289-13	0.244-12	0.174-11	0.928-11
20.....	0.271-12	0.860-12	0.276-11	0.893-11	0.291-10
21.....	0.353-5	0.275-4	0.216-3	0.132-2	0.485-2
22.....	0.637-13	0.196-12	0.581-12	0.160-11	0.427-11
23.....	0.283-13	0.877-13	0.262-12	0.726-12	0.191-11
24.....	0.105-13	0.326-13	0.981-13	0.278-12	0.756-12
25.....	0.557-15	0.276-14	0.172-13	0.109-12	0.565-12
26.....	0.164-14	0.680-14	0.353-13	0.201-12	0.990-12
27.....	0.476-14	0.169-13	0.692-13	0.323-12	0.145-11
28.....	0.138-13	0.448-13	0.152-12	0.550-12	0.202-11
29.....	0.742-13	0.230-12	0.693-12	0.196-11	0.531-11
30.....	0.960-13	0.300-12	0.916-12	0.269-11	0.771-11
31.....	0.179-11	0.554-11	0.164-10	0.449-10	0.115-9
32.....	0.203-13	0.191-12	0.168-11	0.121-10	0.648-10
33.....	0.205-12	0.635-12	0.190-11	0.535-11	0.143-10
34.....	0.259-14	0.151-13	0.106-12	0.705-12	0.366-11
35.....	0.192-13	0.606-13	0.190-12	0.593-12	0.184-11
36.....	0.651-14	0.215-13	0.756-13	0.287-12	0.110-11
37.....	0.708-13	0.220-12	0.671-12	0.195-11	0.548-11
38.....	0.427-13	0.140-12	0.485-12	0.180-11	0.672-11
39.....	0.178-14	0.721-14	0.361-13	0.199-12	0.956-12
40.....	0.814-14	0.283-13	0.112-12	0.492-12	0.209-11

TABLE 5B  
RELATIVE LEVEL POPULATIONS;  $\log T_e = 6.4$

LEVEL <sup>a</sup>	$\log N_e$			
	10.5	11.0	11.5	12.0
1.....	0.438+0	0.383+0	0.363+0	0.357+0
2.....	0.552+0	0.604+0	0.622+0	0.628+0
3.....	0.364-7	0.108-6	0.333-6	0.105-5
4.....	0.383-6	0.120-5	0.378-5	0.120-4
5.....	0.173-6	0.555-6	0.176-5	0.558-5
6.....	0.125-7	0.359-7	0.109-6	0.341-6
7.....	0.170-7	0.574-7	0.186-6	0.591-6
8.....	0.199-8	0.588-8	0.181-7	0.568-7
9.....	0.147-8	0.446-8	0.138-7	0.435-7
10.....	0.235-8	0.775-8	0.248-7	0.789-7
11.....	0.154-8	0.441-8	0.134-7	0.420-7
12.....	0.170-8	0.587-8	0.191-7	0.610-7
13.....	0.777-9	0.229-8	0.707-8	0.222-7
14.....	0.110-8	0.354-8	0.112-7	0.357-7
15.....	0.130-11	0.448-11	0.146-10	0.476-10
16.....	0.101-8	0.289-8	0.876-8	0.274-7
17.....	0.135-8	0.401-8	0.124-7	0.388-7
18.....	0.264-8	0.772-8	0.234-7	0.730-7
19.....	0.373-10	0.129-9	0.420-9	0.134-8
20.....	0.934-10	0.297-9	0.941-9	0.298-8
21.....	0.993-2	0.134-1	0.150-1	0.155-1
22.....	0.124-10	0.388-10	0.123-9	0.389-9
23.....	0.518-11	0.152-10	0.467-10	0.147-9
24.....	0.212-11	0.634-11	0.196-10	0.617-10
25.....	0.228-11	0.793-11	0.259-10	0.832-10
26.....	0.393-11	0.136-10	0.444-10	0.143-9
27.....	0.563-11	0.194-10	0.634-10	0.203-9
28.....	0.705-11	0.233-10	0.749-10	0.239-9
29.....	0.148-10	0.441-10	0.136-9	0.428-9
30.....	0.227-10	0.694-10	0.217-9	0.683-9
31.....	0.303-9	0.874-9	0.267-8	0.834-8
32.....	0.261-9	0.904-9	0.294-8	0.940-8
33.....	0.393-10	0.116-9	0.358-9	0.112-8
34.....	0.146-10	0.506-10	0.165-9	0.526-9
35.....	0.575-11	0.181-10	0.570-10	0.180-9
36.....	0.386-11	0.127-10	0.408-10	0.130-9
37.....	0.158-10	0.479-10	0.149-9	0.469-9
38.....	0.234-10	0.768-10	0.246-9	0.781-9
39.....	0.371-11	0.127-10	0.412-10	0.131-9
40.....	0.776-11	0.261-10	0.843-10	0.268-9

<sup>a</sup> Keyed to Table 1.

and the photographic spectrum of Dere (1982)(D82) covering the same range 170–630 Å, which recorded lines from individual active regions. The observed intensities of Fe XIV lines in these spectra are collected in Table 9. Included in the entries are present identifications of some previously unidentified lines, made possible in part by the measured intensities of D82, which will be seen to be borne out by comparison with the predicted intensities.

The two main categories of known and candidate Fe XIV lines in these spectra are compared with our predicted intensities in Figures 4, 5, and 6. In these figures, in general solid symbols represent previous, positively identified Fe XIV lines, while open symbols represent unidentified lines or lines presently given alternate identifications. Squares represent the MH observations, circles represent BCFD observations, triangles represent the active region observations of D82 and diamonds represent the flare observations of D78. Calculated line intensities are shown by the vertical lines between horizontal bars, which represent the ranges of intensity corresponding to the density range  $\log N_e = 8.0$ –12.0 (approximately the range from quiet Sun to flare densities); in a few cases line ratios (relative

to line  $J$ ) are independent of density so that a single horizontal bar represents their constant value.

There is evidently much information available in these figures. Figure 4 includes the stronger resonance lines, giving a direct comparison with predictions. The first point to be noted is that the photoelectric intensities of MH are in very good agreement with the calculated intensities, differing in all cases by no more than a factor of 2. This shows that the calculated (and observed) values are reliable. A separate point of interest is that the MH values are all in close agreement with the active region values of D82, indicating reliability of the latter's photographic calibration and also source similarities. The next point is that the sets of observations vary systematically with solar excitation conditions, the progression being—from low excitation to high excitation—McMath active region 12375 (D82; inverted triangles); active disk (MH; squares); McMath active region 12390 (D82; upright triangles); active disk (BCFD; circles); and solar flares (D78; diamonds). Another feature worth examining is the varying agreement of the observations with the predicted ranges of variation in line intensities. In some cases, such as lines K, L, and E, there is good

TABLE 6A

Fe XIV LINE<sup>a</sup> RATIOS;<sup>b</sup>  $\log T_e = 6.0$ ,  $\log N_e = 8.0$ 

Line <sup>a</sup>	$-\log R$	Line <sup>a</sup>	$-\log R$	Line <sup>a</sup>	$-\log R$
M .....	0.114+1	l .....	0.274+1	al .....	0.324+1
N .....	0.224+1	m .....	0.358+1	am .....	0.283+1
O .....	0.295+1	n .....	0.465+1	an .....	0.328+1
B .....	0.482+0	o .....	0.292+1	ao .....	0.171+1
I .....	0.584+0	p .....	0.239+1	ap .....	0.373+1
F .....	0.366+0	pp .....	0.321+1	aq .....	0.288+1
G .....	0.101+1	q .....	0.423+1	at .....	0.203+1
J .....	0.000+0	r .....	0.340+1	au .....	0.392+1
P .....	0.262+1	s .....	0.273+1	av .....	0.307+1
Q .....	0.197+1	t .....	0.465+1	aw .....	0.307+1
R .....	0.197+1	u .....	0.190+1	ax .....	0.251+1
C .....	0.180+1	v .....	0.302+1	az .....	0.221+1
A .....	0.120+1	w .....	0.291+1	ba .....	0.409+1
H .....	0.113+1	x .....	0.400+1	bb .....	0.306+1
D .....	0.410+1	y .....	0.321+1	bc .....	0.263+1
E .....	0.404+0	z .....	0.220+1	bd .....	0.344+1
L .....	0.650+0	aa .....	0.298+1	be .....	0.277+1
K .....	0.132+1	ab .....	0.114+1	bf .....	0.386+1
b .....	0.259+1	ac .....	0.330+1	bg .....	0.369+1
c .....	0.286+1	ad .....	0.232+1	bh .....	0.324+1
e .....	0.295+1	ae .....	0.196+1	bi .....	0.437+1
f .....	0.260+1	af .....	0.304+1	bj .....	0.297+1
g .....	0.354+1	ag .....	0.225+1	bk .....	0.284+1
h .....	0.231+1	ah .....	0.323+1	bl .....	0.276+1
i .....	0.427+1	ai .....	0.210+1	bm .....	0.338+1
j .....	0.392+1	aj .....	0.183+1	bn .....	0.563+1
k .....	0.371+1	ak .....	0.290+1		

TABLE 6C

Fe XIV LINE<sup>a</sup> RATIOS;<sup>b</sup>  $\log T_e = 6.0$ ,  $\log N_e = 10.0$ 

Line <sup>a</sup>	$-\log R$	Line <sup>a</sup>	$-\log R$	Line <sup>a</sup>	$-\log R$
M .....	0.146+1	l .....	0.269+1	al .....	0.319+1
N .....	0.218+1	m .....	0.327+1	am .....	0.263+1
O .....	0.281+1	n .....	0.362+1	an .....	0.303+1
B .....	0.475+0	o .....	0.287+1	ao .....	0.166+1
I .....	0.487+0	p .....	0.207+1	ap .....	0.240+1
F .....	0.296+1	pp .....	0.317+1	aq .....	0.283+1
G .....	0.580+1	q .....	0.321+1	at .....	0.193+1
J .....	0.000+0	r .....	0.267+1	au .....	0.301+1
P .....	0.256+1	s .....	0.234+1	av .....	0.277+1
Q .....	0.182+1	t .....	0.297+1	aw .....	0.282+1
R .....	0.161+1	u .....	0.186+1	ax .....	0.246+1
C .....	0.179+1	v .....	0.271+1	az .....	0.179+1
A .....	0.544+0	w .....	0.291+1	ba .....	0.318+1
H .....	0.104+1	x .....	0.238+1	bb .....	0.243+1
D .....	0.340+0	y .....	0.296+1	bc .....	0.262+1
E .....	-0.269-1	z .....	0.213+1	bd .....	0.299+1
L .....	0.650+0	aa .....	0.286+1	be .....	0.267+1
K .....	0.683-1	ab .....	0.113+1	bf .....	0.295+1
b .....	0.256+1	ac .....	0.286+1	bg .....	0.307+1
c .....	0.279+1	ad .....	0.228+1	bh .....	0.323+1
e .....	0.296+1	ae .....	0.165+1	bi .....	0.270+1
f .....	0.255+1	af .....	0.300+1	bj .....	0.278+1
g .....	0.329+1	ag .....	0.200+1	bk .....	0.274+1
h .....	0.227+1	ah .....	0.316+1	bl .....	0.234+1
i .....	0.305+1	ai .....	0.198+1	bm .....	0.276+1
j .....	0.290+1	aj .....	0.182+1	bn .....	0.443+1
k .....	0.299+1	ak .....	0.122+1		

TABLE 6B

Fe XIV LINE<sup>a</sup> RATIOS;<sup>b</sup>  $\log T_e = 6.0$ ,  $\log N_e = 9.0$ 

Line <sup>a</sup>	$-\log R$	Line <sup>a</sup>	$-\log R$	Line <sup>a</sup>	$-\log R$
M .....	0.118+1	l .....	0.273+1	al .....	0.323+1
N .....	0.223+1	m .....	0.351+1	am .....	0.279+1
O .....	0.292+1	n .....	0.422+1	an .....	0.323+1
B .....	0.481+0	o .....	0.291+1	ao .....	0.170+1
I .....	0.566+0	p .....	0.230+1	ap .....	0.308+1
F .....	0.353+0	pp .....	0.321+1	aq .....	0.287+1
G .....	0.901+0	q .....	0.382+1	at .....	0.201+1
J .....	0.000+0	r .....	0.317+1	au .....	0.357+1
P .....	0.261+0	s .....	0.264+1	av .....	0.300+1
Q .....	0.194+1	t .....	0.369+1	aw .....	0.302+1
R .....	0.188+1	u .....	0.190+1	ax .....	0.250+1
C .....	0.179+1	v .....	0.295+1	az .....	0.210+1
A .....	0.994+0	w .....	0.291+1	ba .....	0.374+1
H .....	0.111+1	x .....	0.310+1	bb .....	0.287+1
D .....	0.397+0	y .....	0.315+1	bc .....	0.263+1
E .....	0.293+0	z .....	0.219+1	bd .....	0.333+1
L .....	0.650+0	aa .....	0.296+1	be .....	0.275+1
K .....	0.732+0	ab .....	0.114+1	bf .....	0.351+1
b .....	0.258+1	ac .....	0.319+1	bg .....	0.350+1
c .....	0.284+1	ad .....	0.232+1	bh .....	0.324+1
e .....	0.296+1	ae .....	0.189+1	bi .....	0.342+1
f .....	0.259+1	af .....	0.303+1	bj .....	0.293+1
g .....	0.348+1	ag .....	0.220+1	bk .....	0.282+1
h .....	0.231+1	ah .....	0.322+1	bl .....	0.265+1
i .....	0.371+1	ai .....	0.208+1	bm .....	0.319+1
j .....	0.351+1	aj .....	0.183+1	bn .....	0.482+1
k .....	0.349+1	ak .....	0.195+1		

TABLE 6D

Fe XIV LINE<sup>a</sup> RATIOS;<sup>b</sup>  $\log T_e = 6.0$ ,  $\log N_e = 11.0$ 

Line <sup>a</sup>	$-\log R$	Line <sup>a</sup>	$-\log R$	Line <sup>a</sup>	$-\log R$
M .....	0.221+1	l .....	0.265+1	al .....	0.315+1
N .....	0.214+1	m .....	0.313+1	am .....	0.252+1
O .....	0.271+1	n .....	0.338+1	an .....	0.291+1
B .....	0.469+1	o .....	0.284+1	ao .....	0.163+1
I .....	0.425+1	p .....	0.201+1	ap .....	0.215+1
F .....	0.248+1	pp .....	0.310+1	aq .....	0.280+1
G .....	0.407+0	q .....	0.297+1	at .....	0.186+1
J .....	0.000+0	r .....	0.244+1	au .....	0.278+1
P .....	0.252+1	s .....	0.216+1	av .....	0.262+1
Q .....	0.173+1	t .....	0.272+1	aw .....	0.269+1
R .....	0.147+1	u .....	0.182+1	ax .....	0.243+1
C .....	0.178+1	v .....	0.257+1	az .....	0.162+1
A .....	0.339+0	w .....	0.292+1	ba .....	0.295+1
H .....	0.973+0	x .....	0.214+1	bb .....	0.223+1
D .....	0.293+0	y .....	0.283+1	bc .....	0.261+1
E .....	-0.200+0	z .....	0.208+1	bd .....	0.282+1
L .....	0.650+0	aa .....	0.278+1	be .....	0.260+1
K .....	-0.171+0	ab .....	0.112+1	bf .....	0.272+1
b .....	0.253+1	ac .....	0.268+1	bg .....	0.286+1
c .....	0.274+1	ad .....	0.224+1	bh .....	0.323+1
e .....	0.297+1	ae .....	0.151+1	bi .....	0.245+1
f .....	0.251+1	af .....	0.296+1	bj .....	0.267+1
g .....	0.316+1	ag .....	0.188+1	bk .....	0.268+1
h .....	0.219+1	ah .....	0.311+1	bl .....	0.217+1
i .....	0.280+1	ai .....	0.190+1	bm .....	0.255+1
j .....	0.266+1	aj .....	0.182+1	bn .....	0.498+1
k .....	0.276+1	ak .....	0.975+0		

agreement with the predicted variation within expected observational errors. In other cases such as lines A, B, D, G, H, and I the flare line intensities (*diamonds*) stand out as being higher than predictions by factors of as much as 10, in contrast to the other sets of observations which are reasonably consistent with the predicted ranges. This can be well explained by the appear-

ance of new high-excitation emission lines in the vicinity of the Fe XIV lines, likely to be present in flares. (It is also possible that the intensity of the reference resonance line J may be diminished by opacity effects in the denser flares, a topic which will be studied in later work.)

Weaker observed line candidates are compared with predic-

TABLE 6E

Fe XIV LINE<sup>a</sup> RATIOS;  $\log T_e = 6.0$ ,  $\log N_e = 12.0$ 

Line <sup>a</sup>	$-\log R$	Line <sup>a</sup>	$-\log R$	Line <sup>a</sup>	$-\log R$
M.....	0.318+1	l.....	0.265+1	al.....	0.315+1
N.....	0.213+1	m.....	0.311+1	am.....	0.250+1
O.....	0.269+1	n.....	0.334+1	an.....	0.289+1
B.....	0.468+0	o.....	0.283+1	ao.....	0.162+1
I.....	0.414+0	p.....	0.200+1	ap.....	0.212+1
F.....	0.240+0	pp.....	0.308+1	aq.....	0.279+1
G.....	0.381+0	q.....	0.293+1	at.....	0.185+1
J.....	0.000+0	r.....	0.241+1	au.....	0.275+1
P.....	0.251+1	s.....	0.213+1	av.....	0.260+1
Q.....	0.171+1	t.....	0.269+1	aw.....	0.267+1
R.....	0.144+1	u.....	0.181+1	ax.....	0.242+1
C.....	0.178+1	v.....	0.254+1	az.....	0.159+1
A.....	0.309+0	w.....	0.292+1	ba.....	0.292+1
H.....	0.962+0	x.....	0.210+1	bb.....	0.220+1
D.....	0.284+0	y.....	0.281+1	bc.....	0.261+1
E.....	-0.226+0	z.....	0.208+1	bd.....	0.279+1
L.....	0.650+0	aa.....	0.277+1	be.....	0.259+1
K.....	-0.205+0	ab.....	0.112+1	bf.....	0.269+1
b.....	0.252+1	ac.....	0.265+1	bg.....	0.283+1
c.....	0.273+1	ad.....	0.223+1	bh.....	0.323+1
e.....	0.297+1	ae.....	0.149+1	bi.....	0.241+1
f.....	0.251+1	af.....	0.295+1	bj.....	0.265+1
g.....	0.314+1	ag.....	0.186+1	bk.....	0.266+1
h.....	0.217+1	ah.....	0.310+1	bl.....	0.214+1
i.....	0.276+1	ai.....	0.189+1	bm.....	0.252+1
j.....	0.262+1	aj.....	0.181+1	bn.....	0.592+1
k.....	0.273+1	ak.....	0.941+0		

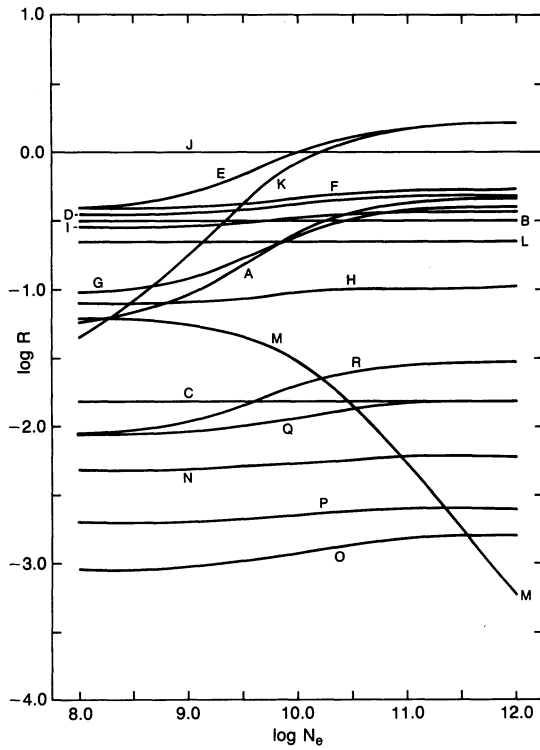
<sup>a</sup> Keyed to Table 2A.<sup>b</sup>  $R = I_{\text{line}}/I_{211.3}$ .

FIG. 1.—Calculated intensity dependence, on electron density  $N_e$ , of Fe XIV resonance lines A–L, forbidden line M, and intercombination lines N–R, relative to line J (211.3 Å);  $\log T_e = 6.2$ . All lines terminate on ground levels 1 or 2 [ $3p(2P_{1/2, 3/2})$ ]. In this and all following figures,  $R \equiv I_\lambda/I_{211.3}$ .

TABLE 7A

Fe XIV LINE<sup>a</sup> RATIOS;  $\log T_e = 6.2$ ,  $\log N_e = 8.0$ 

Line <sup>a</sup>	$-\log R$	Line <sup>a</sup>	$-\log R$	Line <sup>a</sup>	$-\log R$
M.....	0.122+1	l.....	0.275+1	al.....	0.319+1
N.....	0.232+1	m.....	0.359+1	am.....	0.283+1
O.....	0.305+1	n.....	0.471+1	an.....	0.328+1
B.....	0.499+0	o.....	0.297+1	ao.....	0.166+1
I.....	0.548+0	p.....	0.244+1	ap.....	0.372+1
F.....	0.414+0	pp.....	0.325+1	aq.....	0.290+1
G.....	0.103+1	q.....	0.426+1	at.....	0.197+1
J.....	0.000+0	r.....	0.343+1	au.....	0.390+1
P.....	0.270+1	s.....	0.276+1	av.....	0.309+1
Q.....	0.207+1	t.....	0.464+1	aw.....	0.307+1
R.....	0.205+1	u.....	0.192+1	ax.....	0.246+1
C.....	0.181+1	v.....	0.303+1	az.....	0.215+1
A.....	0.124+1	w.....	0.295+1	ba.....	0.407+1
H.....	0.110+1	x.....	0.402+1	bb.....	0.301+1
D.....	0.458+0	y.....	0.320+1	bc.....	0.260+1
E.....	0.418+0	z.....	0.218+1	bd.....	0.344+1
L.....	0.650+0	aa.....	0.296+1	be.....	0.271+1
K.....	0.135+1	ab.....	0.111+1	bf.....	0.384+1
b.....	0.263+1	ac.....	0.330+1	bg.....	0.365+1
c.....	0.289+1	ad.....	0.234+1	bh.....	0.321+1
e.....	0.300+1	ae.....	0.197+1	bi.....	0.437+1
f.....	0.265+1	af.....	0.309+1	bj.....	0.297+1
g.....	0.353+1	ag.....	0.225+1	bk.....	0.278+1
h.....	0.234+1	ah.....	0.321+1	bl.....	0.270+1
i.....	0.432+1	ai.....	0.208+1	bm.....	0.334+1
j.....	0.395+1	aj.....	0.180+1	bn.....	0.570+1
k.....	0.375+1	ak.....	0.289+1		

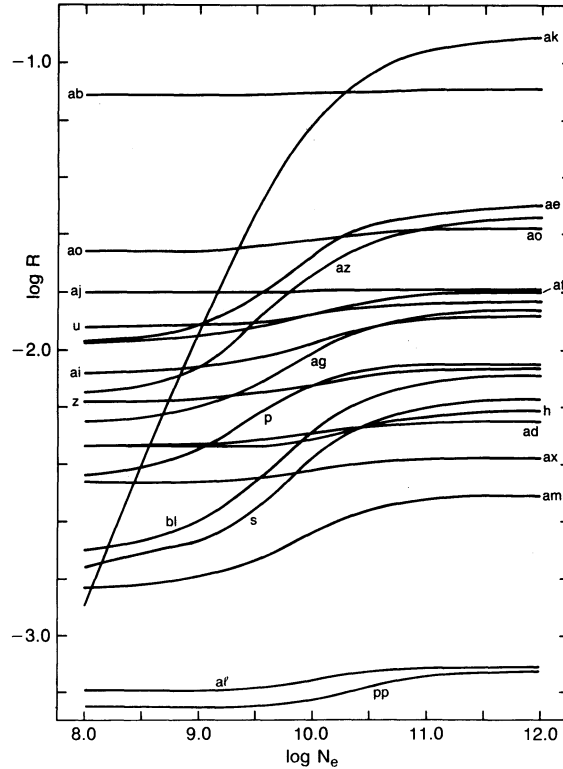


FIG. 2.—Calculated relative intensity dependence, on electron density  $N_e$ , of 20 stronger Fe XIV subordinate lines terminating on levels above the ground levels; intensities relative to line J (211.3 Å);  $\log T_e = 6.2$ .

TABLE 7B

Fe XIV LINE<sup>a</sup> RATIOS;<sup>b</sup>  $\log T_e = 6.2$ ,  $\log N_e = 9.0$ 

Line <sup>a</sup>	$-\log R$	Line <sup>a</sup>	$-\log R$	Line <sup>a</sup>	$-\log R$
M .....	0.126+1	l .....	0.274+1	al .....	0.319+1
N .....	0.231+1	m .....	0.353+1	am .....	0.279+1
O .....	0.303+1	n .....	0.427+1	an .....	0.323+1
B .....	0.499+0	o .....	0.296+1	ao .....	0.166+1
I .....	0.537+0	p .....	0.235+1	ap .....	0.306+1
F .....	0.399+0	pp .....	0.325+1	aq .....	0.289+1
G .....	0.921+0	q .....	0.387+1	at .....	0.195+1
J .....	0.000+0	r .....	0.321+1	au .....	0.354+1
P .....	0.269+1	s .....	0.267+1	av .....	0.302+1
Q .....	0.204+1	t .....	0.368+1	aw .....	0.301+1
R .....	0.197+1	u .....	0.191+1	ax .....	0.246+1
C .....	0.181+1	v .....	0.296+1	az .....	0.205+1
A .....	0.104+1	w .....	0.296+1	ba .....	0.372+1
H .....	0.109+1	x .....	0.312+1	bb .....	0.283+1
D .....	0.440+0	y .....	0.315+1	bc .....	0.260+1
E .....	0.313+0	z .....	0.217+1	bd .....	0.333+1
L .....	0.650+0	aa .....	0.294+1	be .....	0.269+1
K .....	0.750+0	ab .....	0.111+1	bf .....	0.349+1
b .....	0.262+1	ac .....	0.319+1	bg .....	0.346+1
c .....	0.288+1	ad .....	0.233+1	bh .....	0.321+1
e .....	0.300+1	ae .....	0.191+1	bi .....	0.341+1
f .....	0.264+1	af .....	0.308+1	bj .....	0.293+1
g .....	0.348+1	ag .....	0.220+1	bk .....	0.277+1
h .....	0.234+1	ah .....	0.320+1	bl .....	0.260+1
i .....	0.377+1	ai .....	0.206+1	bm .....	0.315+1
j .....	0.356+1	aj .....	0.180+1	bn .....	0.488+1
k .....	0.353+1	ak .....	0.194+1		

TABLE 7C

Fe XIV LINE<sup>a</sup> RATIOS;<sup>b</sup>  $\log T_e = 6.2$ ,  $\log N_e = 10.0$ 

Line <sup>a</sup>	$-\log R$	Line <sup>a</sup>	$-\log R$	Line <sup>a</sup>	$-\log R$
M .....	0.152+1	l .....	0.270+1	al .....	0.315+1
N .....	0.226+1	m .....	0.329+1	am .....	0.264+1
O .....	0.291+1	n .....	0.365+1	an .....	0.304+1
B .....	0.498+0	o .....	0.292+1	ao .....	0.162+1
I .....	0.485+0	p .....	0.212+1	ap .....	0.237+1
F .....	0.334+0	pp .....	0.322+1	aq .....	0.285+1
G .....	0.606+0	q .....	0.326+1	at .....	0.187+1
J .....	0.000+0	r .....	0.272+1	au .....	0.297+1
P .....	0.264+1	s .....	0.238+1	av .....	0.279+1
Q .....	0.193+1	t .....	0.295+1	aw .....	0.282+1
R .....	0.170+1	u .....	0.187+1	ax .....	0.242+1
C .....	0.181+1	v .....	0.273+1	az .....	0.174+1
A .....	0.582+0	w .....	0.296+1	ba .....	0.314+1
H .....	0.103+1	x .....	0.239+1	bb .....	0.239+1
D .....	0.378+0	y .....	0.296+1	bc .....	0.259+1
E .....	-0.155-2	z .....	0.212+1	bd .....	0.300+1
L .....	0.650+0	aa .....	0.285+1	be .....	0.262+1
K .....	0.763-1	ab .....	0.110+1	bf .....	0.291+1
b .....	0.259+1	ac .....	0.286+1	bg .....	0.302+1
c .....	0.283+1	ad .....	0.229+1	bh .....	0.320+1
e .....	0.301+1	ae .....	0.167+1	bi .....	0.268+1
f .....	0.260+1	af .....	0.305+1	bj .....	0.278+1
g .....	0.329+1	ag .....	0.201+1	bk .....	0.269+1
h .....	0.231+1	ah .....	0.315+1	bl .....	0.229+1
i .....	0.310+1	ai .....	0.197+1	bm .....	0.271+1
j .....	0.295+1	aj .....	0.179+1	bn .....	0.442+1
k .....	0.304+1	ak .....	0.120+1		

TABLE 7D

Fe XIV LINE<sup>a</sup> RATIOS;<sup>b</sup>  $\log T_e = 6.2$ ,  $\log N_e = 11.0$ 

Line <sup>a</sup>	$-\log R$	Line <sup>a</sup>	$-\log R$	Line <sup>a</sup>	$-\log R$
M .....	0.227+1	l .....	0.267+1	al .....	0.311+1
N .....	0.222+1	m .....	0.315+1	am .....	0.252+1
O .....	0.281+1	n .....	0.340+1	an .....	0.291+1
B .....	0.497+0	o .....	0.289+1	ao .....	0.158+1
I .....	0.440+0	p .....	0.205+1	ap .....	0.212+1
F .....	0.278+0	pp .....	0.314+1	aq .....	0.282+1
G .....	0.429+0	q .....	0.301+1	at .....	0.181+1
J .....	0.000+0	r .....	0.249+1	au .....	0.273+1
P .....	0.260+1	s .....	0.220+1	av .....	0.264+1
Q .....	0.183+1	t .....	0.269+1	aw .....	0.269+1
R .....	0.155+1	u .....	0.184+1	ax .....	0.238+1
C .....	0.181+1	v .....	0.258+1	az .....	0.157+1
A .....	0.370+0	w .....	0.297+1	ba .....	0.290+1
H .....	0.988+0	x .....	0.214+1	bb .....	0.218+1
D .....	0.323+0	y .....	0.283+1	bc .....	0.259+1
E .....	-0.178+0	z .....	0.207+1	bd .....	0.282+1
L .....	0.650+0	aa .....	0.277+1	be .....	0.255+1
K .....	-0.171+0	ab .....	0.109+1	bf .....	0.267+1
b .....	0.257+1	ac .....	0.268+1	bg .....	0.282+1
c .....	0.278+1	ad .....	0.226+1	bh .....	0.320+1
e .....	0.302+1	ae .....	0.153+1	bi .....	0.242+1
f .....	0.257+1	af .....	0.320+1	bj .....	0.267+1
g .....	0.316+1	ag .....	0.188+1	bk .....	0.262+1
h .....	0.223+1	ah .....	0.310+1	bl .....	0.211+1
i .....	0.284+1	ai .....	0.189+1	bm .....	0.251+1
j .....	0.270+1	aj .....	0.179+1	bn .....	0.492+1
k .....	0.280+1	ak .....	0.949+0		

TABLE 7E

Fe XIV LINE<sup>a</sup> RATIOS;<sup>b</sup>  $\log T_e = 6.2$ ,  $\log N_e = 12.0$ 

Line <sup>a</sup>	$-\log R$	Line <sup>a</sup>	$-\log R$	Line <sup>a</sup>	$-\log R$
M .....	0.323+1	l .....	0.266+1	al .....	0.311+1
N .....	0.222+1	m .....	0.312+1	am .....	0.251+1
O .....	0.279+1	n .....	0.336+1	an .....	0.288+1
B .....	0.497+0	o .....	0.288+1	ao .....	0.158+1
I .....	0.432+0	p .....	0.205+1	ap .....	0.208+1
F .....	0.268+0	pp .....	0.312+1	aq .....	0.281+1
G .....	0.402+0	q .....	0.298+1	at .....	0.180+1
J .....	0.000+0	r .....	0.245+1	au .....	0.270+1
P .....	0.260+1	s .....	0.217+1	av .....	0.262+1
Q .....	0.181+1	t .....	0.266+1	aw .....	0.267+1
R .....	0.153+1	u .....	0.183+1	ax .....	0.238+1
C .....	0.181+1	v .....	0.256+1	az .....	0.154+1
A .....	0.338+0	w .....	0.297+1	ba .....	0.287+1
H .....	0.980+0	x .....	0.211+1	bb .....	0.215+1
D .....	0.313+0	y .....	0.281+1	bc .....	0.258+1
E .....	-0.205+0	z .....	0.206+1	bd .....	0.279+1
L .....	0.650+0	aa .....	0.276+1	be .....	0.254+1
K .....	-0.206+0	ab .....	0.109+1	bf .....	0.264+1
b .....	0.256+1	ac .....	0.265+1	bg .....	0.278+1
c .....	0.277+1	ad .....	0.225+1	bh .....	0.320+1
e .....	0.302+1	ae .....	0.150+1	bi .....	0.239+1
f .....	0.256+1	af .....	0.300+1	bj .....	0.265+1
g .....	0.314+1	ag .....	0.186+1	bk .....	0.261+1
h .....	0.221+1	ah .....	0.309+1	bl .....	0.209+1
i .....	0.280+1	ai .....	0.188+1	bm .....	0.247+1
j .....	0.266+1	aj .....	0.179+1	bn .....	0.585+1
k .....	0.276+1	ak .....	0.913+0		

<sup>a</sup> Keyed to Table 2A.<sup>b</sup>  $R \equiv I_{\text{Line}}/I_{211.3}$ .

field line feature in the MH spectrum with transition *ag*. The line feature in the vicinity of 225.48 Å listed in the flare spectrum of D78, if real, is apparently not due to line *aj*. On the other hand, the D82 observation of a line at 447.36 Å is verified to be the intercombination line *R*.

In the course of assembling this paper, results of the GSFC-

TABLE 8A

Fe XIV LINE<sup>a</sup> RATIOS,<sup>b</sup>  $\log T_e = 6.4$ ,  $\log N_e = 8.0$ 

Line <sup>a</sup>	-log R	Line <sup>a</sup>	-log R	Line <sup>a</sup>	-log R
M .....	0.126+1	<i>l</i> .....	0.277+1	<i>al</i> .....	0.318+1
N .....	0.238+1	<i>m</i> .....	0.362+1	<i>am</i> .....	0.283+1
O .....	0.314+1	<i>n</i> .....	0.476+1	<i>an</i> .....	0.329+1
B .....	0.514+0	<i>o</i> .....	0.301+1	<i>ao</i> .....	0.165+1
I .....	0.524+0	<i>p</i> .....	0.248+1	<i>ap</i> .....	0.373+1
F .....	0.452+0	<i>pp</i> .....	0.328+1	<i>aq</i> .....	0.292+1
G .....	0.104+0	<i>q</i> .....	0.430+1	<i>at</i> .....	0.195+1
J .....	0.000+0	<i>r</i> .....	0.346+1	<i>au</i> .....	0.390+1
P .....	0.276+1	<i>s</i> .....	0.279+1	<i>av</i> .....	0.311+1
Q .....	0.216+1	<i>t</i> .....	0.467+1	<i>aw</i> .....	0.308+1
R .....	0.212+1	<i>u</i> .....	0.194+1	<i>ax</i> .....	0.245+1
C .....	0.183+1	<i>v</i> .....	0.306+1	<i>az</i> .....	0.214+1
A .....	0.128+1	<i>w</i> .....	0.300+1	<i>ba</i> .....	0.407+1
H .....	0.107+1	<i>x</i> .....	0.407+1	<i>bb</i> .....	0.300+1
D .....	0.496+0	<i>y</i> .....	0.322+1	<i>bc</i> .....	0.260+1
E .....	0.429+0	<i>z</i> .....	0.218+1	<i>bd</i> .....	0.344+1
L .....	0.650+0	<i>aa</i> .....	0.296+1	<i>be</i> .....	0.269+1
K .....	0.139+1	<i>ab</i> .....	0.111+1	<i>bf</i> .....	0.384+1
b .....	0.266+1	<i>ac</i> .....	0.331+1	<i>bg</i> .....	0.364+1
c .....	0.292+1	<i>ad</i> .....	0.236+1	<i>bh</i> .....	0.321+1
e .....	0.304+1	<i>ae</i> .....	0.200+1	<i>bi</i> .....	0.440+1
f .....	0.269+1	<i>af</i> .....	0.313+1	<i>bj</i> .....	0.298+1
g .....	0.354+1	<i>ag</i> .....	0.226+1	<i>bk</i> .....	0.277+1
h .....	0.237+1	<i>ah</i> .....	0.321+1	<i>bl</i> .....	0.268+1
i .....	0.436+1	<i>ai</i> .....	0.209+1	<i>bm</i> .....	0.333+1
j .....	0.399+1	<i>aj</i> .....	0.180+1	<i>bn</i> .....	0.577+1
k .....	0.378+1	<i>ak</i> .....	0.293+1		

TABLE 8B

Fe XIV LINE<sup>a</sup> RATIOS,<sup>b</sup>  $\log T_e = 6.4$ ,  $\log N_e = 9.0$ 

Line <sup>a</sup>	-log R	Line <sup>a</sup>	-log R	Line <sup>a</sup>	-log R
M .....	0.130+1	<i>l</i> .....	0.277+1	<i>al</i> .....	0.317+1
N .....	0.237+1	<i>m</i> .....	0.356+1	<i>am</i> .....	0.280+1
O .....	0.312+1	<i>n</i> .....	0.432+1	<i>an</i> .....	0.324+1
B .....	0.515+0	<i>o</i> .....	0.300+1	<i>ao</i> .....	0.165+1
I .....	0.517+0	<i>p</i> .....	0.239+1	<i>ap</i> .....	0.308+1
F .....	0.436+0	<i>pp</i> .....	0.328+1	<i>aq</i> .....	0.291+1
G .....	0.939+0	<i>q</i> .....	0.393+1	<i>at</i> .....	0.193+1
J .....	0.000+0	<i>r</i> .....	0.326+1	<i>au</i> .....	0.355+1
P .....	0.275+1	<i>s</i> .....	0.271+1	<i>av</i> .....	0.305+1
Q .....	0.213+1	<i>t</i> .....	0.372+1	<i>aw</i> .....	0.303+1
R .....	0.204+1	<i>u</i> .....	0.194+1	<i>ax</i> .....	0.245+1
C .....	0.183+1	<i>v</i> .....	0.300+1	<i>az</i> .....	0.204+1
A .....	0.109+1	<i>w</i> .....	0.300+1	<i>ba</i> .....	0.376+1
H .....	0.107+1	<i>x</i> .....	0.317+1	<i>bb</i> .....	0.282+1
D .....	0.481+0	<i>y</i> .....	0.317+1	<i>bc</i> .....	0.260+1
E .....	0.332+0	<i>z</i> .....	0.217+1	<i>bd</i> .....	0.334+1
L .....	0.650+0	<i>aa</i> .....	0.295+1	<i>be</i> .....	0.268+1
K .....	0.784+0	<i>ab</i> .....	0.111+1	<i>bf</i> .....	0.349+1
b .....	0.265+1	<i>ac</i> .....	0.320+1	<i>bg</i> .....	0.346+1
c .....	0.291+1	<i>ad</i> .....	0.235+1	<i>bh</i> .....	0.321+1
e .....	0.305+1	<i>ae</i> .....	0.194+1	<i>bi</i> .....	0.345+1
f .....	0.268+1	<i>af</i> .....	0.312+1	<i>bj</i> .....	0.294+1
g .....	0.350+1	<i>ag</i> .....	0.222+1	<i>bk</i> .....	0.275+1
h .....	0.237+1	<i>ah</i> .....	0.320+1	<i>bl</i> .....	0.259+1
i .....	0.383+1	<i>ai</i> .....	0.207+1	<i>bm</i> .....	0.315+1
j .....	0.362+1	<i>aj</i> .....	0.180+1	<i>bn</i> .....	0.494+1
k .....	0.358+1	<i>ak</i> .....	0.197+1		

TABLE 8C

Fe XIV LINE<sup>a</sup> RATIOS,<sup>b</sup>  $\log T_e = 6.4$ ,  $\log N_e = 10.0$ 

Line <sup>a</sup>	-log R	Line <sup>a</sup>	-log R	Line <sup>a</sup>	-log R
M .....	0.155+1	<i>l</i> .....	0.273+1	<i>al</i> .....	0.314+1
N .....	0.233+1	<i>m</i> .....	0.333+1	<i>am</i> .....	0.265+1
O .....	0.300+1	<i>n</i> .....	0.369+1	<i>an</i> .....	0.306+1
B .....	0.518+0	<i>o</i> .....	0.297+1	<i>ao</i> .....	0.161+1
I .....	0.483+0	<i>p</i> .....	0.216+1	<i>ap</i> .....	0.238+1
F .....	0.364+0	<i>pp</i> .....	0.325+1	<i>aq</i> .....	0.288+1
G .....	0.631+0	<i>q</i> .....	0.332+1	<i>at</i> .....	0.186+1
J .....	0.000+0	<i>r</i> .....	0.278+1	<i>au</i> .....	0.297+1
P .....	0.271+1	<i>s</i> .....	0.243+1	<i>av</i> .....	0.282+1
Q .....	0.202+1	<i>t</i> .....	0.297+1	<i>aw</i> .....	0.285+1
R .....	0.178+1	<i>u</i> .....	0.190+1	<i>ax</i> .....	0.241+1
C .....	0.183+1	<i>v</i> .....	0.277+1	<i>az</i> .....	0.174+1
A .....	0.625+1	<i>w</i> .....	0.300+1	<i>ba</i> .....	0.314+1
H .....	0.103+1	<i>x</i> .....	0.243+1	<i>bb</i> .....	0.239+1
D .....	0.408+0	<i>y</i> .....	0.298+1	<i>bc</i> .....	0.259+1
E .....	0.235-1	<i>z</i> .....	0.213+1	<i>bd</i> .....	0.302+1
L .....	0.650+0	<i>aa</i> .....	0.286+1	<i>be</i> .....	0.260+1
K .....	0.947-1	<i>ab</i> .....	0.110+1	<i>bf</i> .....	0.291+1
b .....	0.263+1	<i>ac</i> .....	0.288+1	<i>bg</i> .....	0.302+1
c .....	0.286+1	<i>ad</i> .....	0.232+1	<i>bh</i> .....	0.320+1
e .....	0.305+1	<i>ae</i> .....	0.171+1	<i>bi</i> .....	0.270+1
f .....	0.265+1	<i>af</i> .....	0.309+1	<i>bj</i> .....	0.279+1
g .....	0.331+1	<i>ag</i> .....	0.203+1	<i>bk</i> .....	0.267+1
h .....	0.235+1	<i>ah</i> .....	0.315+1	<i>bl</i> .....	0.229+1
i .....	0.315+1	<i>ai</i> .....	0.198+1	<i>bm</i> .....	0.271+1
j .....	0.301+1	<i>aj</i> .....	0.179+1	<i>bn</i> .....	0.443+1
k .....	0.309+1	<i>ak</i> .....	0.122+1		

TABLE 8D

Fe XIV LINE<sup>a</sup> RATIOS,<sup>b</sup>  $\log T_e = 6.4$ ,  $\log N_e = 11.0$ 

Line <sup>a</sup>	-log R	Line <sup>a</sup>	-log R	Line <sup>a</sup>	-log R
M .....	0.228+1	<i>l</i> .....	0.270+1	<i>al</i> .....	0.310+1
N .....	0.229+1	<i>m</i> .....	0.318+1	<i>am</i> .....	0.253+1
O .....	0.290+1	<i>n</i> .....	0.344+1	<i>an</i> .....	0.293+1
B .....	0.520+0	<i>o</i> .....	0.293+1	<i>ao</i> .....	0.157+1
I .....	0.450+0	<i>p</i> .....	0.209+1	<i>ap</i> .....	0.211+1
F .....	0.300+0	<i>pp</i> .....	0.317+1	<i>aq</i> .....	0.284+1
G .....	0.446+0	<i>q</i> .....	0.305+1	<i>at</i> .....	0.179+1
J .....	0.000+0	<i>r</i> .....	0.253+1	<i>au</i> .....	0.272+1
P .....	0.267+1	<i>s</i> .....	0.224+1	<i>av</i> .....	0.267+1
Q .....	0.191+1	<i>t</i> .....	0.270+1	<i>aw</i> .....	0.271+1
R .....	0.162+1	<i>u</i> .....	0.186+1	<i>ax</i> .....	0.237+1
C .....	0.183+1	<i>v</i> .....	0.262+1	<i>az</i> .....	0.155+1
A .....	0.400+0	<i>w</i> .....	0.301+1	<i>ba</i> .....	0.289+1
H .....	0.998+0	<i>x</i> .....	0.216+1	<i>bb</i> .....	0.217+1
D .....	0.344+0	<i>y</i> .....	0.285+1	<i>bc</i> .....	0.259+1
E .....	-0.161+0	<i>z</i> .....	0.208+1	<i>bd</i> .....	0.283+1
L .....	0.650+0	<i>aa</i> .....	0.278+1	<i>be</i> .....	0.254+1
K .....	-0.167+0	<i>ab</i> .....	0.109+1	<i>bf</i> .....	0.266+1
b .....	0.260+1	<i>ac</i> .....	0.269+1	<i>bg</i> .....	0.280+1
c .....	0.282+1	<i>ad</i> .....	0.228+1	<i>bh</i> .....	0.320+1
e .....	0.306+1	<i>ae</i> .....	0.156+1	<i>bi</i> .....	0.243+1
f .....	0.261+1	<i>af</i> .....	0.305+1	<i>bj</i> .....	0.268+1
g .....	0.318+1	<i>ag</i> .....	0.190+1	<i>bk</i> .....	0.261+1
h .....	0.226+1	<i>ah</i> .....	0.311+1	<i>bl</i> .....	0.210+1
i .....	0.288+1	<i>ai</i> .....	0.190+1	<i>bm</i> .....	0.249+1
j .....	0.274+1	<i>aj</i> .....	0.179+1	<i>bn</i> .....	0.486+1
k .....	0.284+1	<i>ak</i> .....	0.954+0		

the relative intensities of the SERTS-identified Fe XIV lines. Also included in Table 10 are the SERTS-measured relative intensities of two line features at 290.69 Å and 358.67 Å which are ascribed presently to Si IX and Fe XI but which as noted above coincide in wavelength with Fe XIV transitions *ag* and *ae* (see Discussion below). These recent measurements are

SERTS (Solar EUV Rocket Telescope and Spectrograph) flight of 1989 May 5, have been made available (Thomas & Neupert 1993) which cover the range 170 to 450 Å photographically and include Fe XIV lines observed in a single active region. The intensities have been photometrically calibrated to within a factor of  $\pm 25\%$  ( $\pm 0.1$  dex) in relative accuracy. Table 10 lists

TABLE 8E

Fe XIV LINE<sup>a</sup> RATIOS;<sup>b</sup>  $\log T_e = 6.4$ ,  $\log N_e = 12.0$ 

Line <sup>a</sup>	$-\log R$	Line <sup>a</sup>	$-\log R$	Line <sup>a</sup>	$-\log R$
<i>M</i> .....	0.324+1	<i>l</i> .....	0.269+1	<i>al</i> .....	0.310+1
<i>N</i> .....	0.228+1	<i>m</i> .....	0.315+1	<i>am</i> .....	0.251+1
<i>O</i> .....	0.288+1	<i>n</i> .....	0.339+1	<i>an</i> .....	0.290+1
<i>B</i> .....	0.521+0	<i>o</i> .....	0.292+1	<i>ao</i> .....	0.157+1
<i>I</i> .....	0.444+0	<i>p</i> .....	0.210+1	<i>ap</i> .....	0.207+1
<i>F</i> .....	0.288+0	<i>pp</i> .....	0.315+1	<i>aq</i> .....	0.284+1
<i>G</i> .....	0.417+0	<i>q</i> .....	0.301+1	<i>at</i> .....	0.178+1
<i>J</i> .....	0.000+0	<i>r</i> .....	0.248+1	<i>au</i> .....	0.268+1
<i>P</i> .....	0.267+1	<i>s</i> .....	0.221+1	<i>av</i> .....	0.264+1
<i>Q</i> .....	0.189+1	<i>t</i> .....	0.266+1	<i>aw</i> .....	0.269+1
<i>R</i> .....	0.160+1	<i>u</i> .....	0.186+1	<i>ax</i> .....	0.237+1
<i>C</i> .....	0.183+1	<i>v</i> .....	0.259+1	<i>az</i> .....	0.153+1
<i>A</i> .....	0.366+0	<i>w</i> .....	0.301+1	<i>ba</i> .....	0.286+1
<i>H</i> .....	0.992+0	<i>x</i> .....	0.213+1	<i>bb</i> .....	0.213+1
<i>D</i> .....	0.332+0	<i>y</i> .....	0.283+1	<i>bc</i> .....	0.258+1
<i>E</i> .....	-0.191+0	<i>z</i> .....	0.207+1	<i>bd</i> .....	0.280+1
<i>L</i> .....	0.650+0	<i>aa</i> .....	0.277+1	<i>be</i> .....	0.252+1
<i>K</i> .....	-0.206+0	<i>ab</i> .....	0.109+1	<i>bf</i> .....	0.263+1
<i>b</i> .....	0.260+1	<i>ac</i> .....	0.266+1	<i>bg</i> .....	0.277+1
<i>c</i> .....	0.281+1	<i>ad</i> .....	0.228+1	<i>bh</i> .....	0.320+1
<i>e</i> .....	0.306+1	<i>ae</i> .....	0.153+1	<i>bi</i> .....	0.239+1
<i>f</i> .....	0.206+1	<i>af</i> .....	0.305+1	<i>bj</i> .....	0.266+1
<i>g</i> .....	0.316+1	<i>ag</i> .....	0.187+1	<i>bk</i> .....	0.260+1
<i>h</i> .....	0.224+1	<i>ah</i> .....	0.310+1	<i>bl</i> .....	0.207+1
<i>i</i> .....	0.284+1	<i>ai</i> .....	0.189+1	<i>bm</i> .....	0.246+1
<i>j</i> .....	0.270+1	<i>aj</i> .....	0.179+1	<i>bn</i> .....	0.578+1
<i>k</i> .....	0.280+1	<i>ak</i> .....	0.915+0		

<sup>a</sup> Keyed to Table 2A.<sup>b</sup>  $R \equiv I_{\text{line}}/I_{211.3}$ .

included in Figures 4 and 5 as circled points. One sees in Figure 4 that agreement with predictions for the resonance lines is again consistently good. In Figure 5, there is very good agreement also with predictions for the weaker lines; line *R* is again verified as present, and line *C* is verified as observed for the first time. The observed line features at 290.7 Å and 358.67 Å in active regions are now seen to be due mainly to Fe XIV transitions *ag* and *ae* rather than the present classifications of Si IX and Fe XI.

It is seen that the SERTS-observed line at 363.75 Å ascribed to Mg VII is accounted for in intensity by the Fe XIV transition (*ad*) expected at this wavelength (Table 2A), and we verify the SERTS identifications of the intercombination lines *N* and *O*, all agreeing with the intensity predictions to within a factor of 2.

It is interesting to find that the intercombination line *Q* at 467.40 Å, not present in any of these solar lists because of sensitivity or wavelength limitations, is included in the D82 list of unidentified lines; its observed relative intensity in McMath active region 12686 is marked on Figure 5 by a cross. In this list we note also that the lines at 239.03 Å and 374.10 Å are probably due to Ni XVI and Ca VIII, respectively, as proposed by SK, coinciding in wavelength with aluminum-like lines listed by RL; and the line at 225.48 Å has been identified by D78 as due to S XII.

As mentioned above, the BCFD-observed line intensity at 218.18 Å is in reasonable agreement with that expected for Fe XIV transition *ak* so that the S XII contribution, if present in active regions, is minor. We note that one of the Fe XIV lines observed by Levashov, Ryabtsev, & Churilov (1990), transition *i* at 212.35 Å, is also present in the BCFD spectrum. The flare-observed line at 225.48 Å on the other hand appears to be due to a different source than transition *aj*.

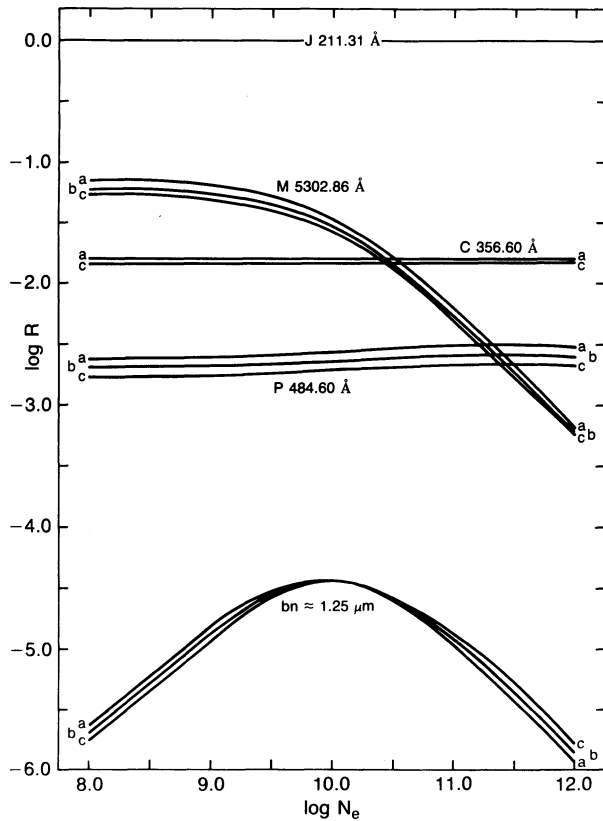


FIG. 3.—Calculated relative intensity dependence, on electron density  $N_e$ , of selected Fe XIV lines: resonance line *C*, intercombination line *P*, magnetic dipole forbidden line *M* and magnetic dipole forbidden line *bn* originating in the high level 21 [ $3s3p3d^4F_{9/2}$ ]. Curves *a*, *b*, *c* correspond, respectively, to  $\log T_e = 6.0, 6.2, 6.4$ . Temperature dependence of the lines is seen to be slight compared to density dependence, at temperatures above  $T_e \approx 10^6$  K. The contrast between the density dependences of the two forbidden lines *M* and *bn* is discussed in the text.

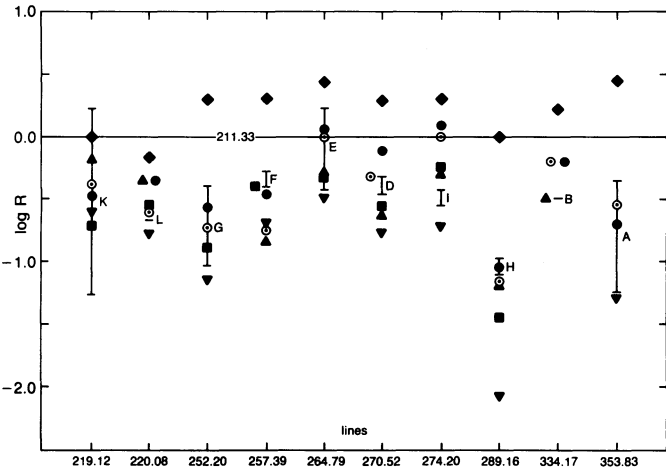


FIG. 4.—Comparison of observed Fe XIV resonance line intensities with predicted intensities. Predicted intensity ranges for  $\log N_e = 8.0-12.0$  are represented by vertical line segments between short horizontal bars; the density-independent (relative) intensities of lines *B*, *L* are represented by single horizontal bars. Solid circles: BCFD, whole active Sun; solid diamonds: D78, flares; upright triangles: D82, McMath active region 12390; inverted triangles: D82, McMath active region 12375; solid squares: MH, whole active Sun; circled points: SERTS, active region NOAA 5464.

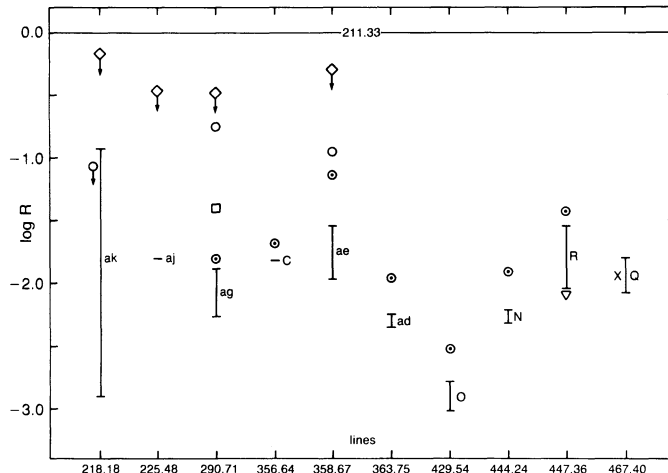


FIG. 5.—Comparison of observed candidate solar line intensities with predicted intensities: open circles, unidentified lines in BCFD list; open diamonds, unidentified lines in D78 flare list; open square, present identification in published spectrum of MH; circled points, SERTS observations; open triangle and cross, unidentified lines in D82 list.

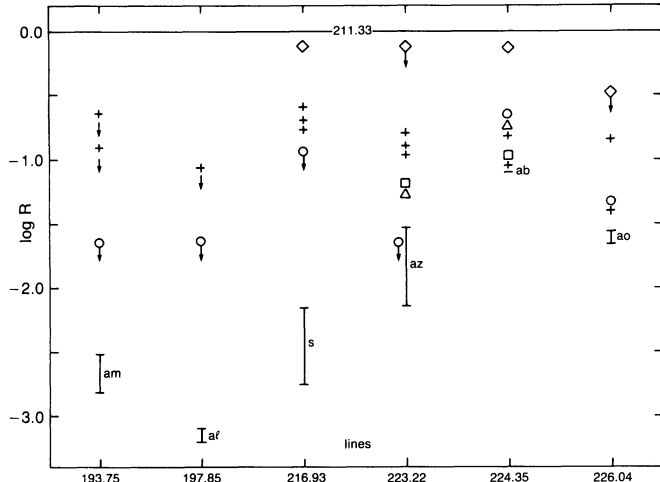


FIG. 6.—Comparison of shorter wavelength candidate solar line intensities with predicted intensities: open circles, unidentified lines in BCFD list; open diamonds, unidentified lines in D78 flare list; open squares, present identifications in published spectrum of MH; open triangles, unidentified lines in D82 list; crosses, present measurements in archival S082A data.

TABLE 9  
OBSERVED RELATIVE INTENSITIES<sup>a</sup> OF Fe XIV LINES<sup>b</sup>

LINE	(Å)	MH <sup>c</sup>	BCFD <sup>d</sup>	D78 <sup>e</sup>	D82 <sup>f</sup>	
					McMath 12390	McMath 12375
R .....	447.36	g	...	h	...	-2.08 <sup>h</sup>
ae ....	358.67	g	-0.95 <sup>i</sup>	< -0.30 <sup>j,l</sup>	...	
A .....	353.83	g	-0.70	+0.43 <sup>j</sup>	...	-1.28
B .....	334.17	g	-0.18	+0.22	-0.52	
ag ....	290.71	-1.4 <sup>h,k,m</sup>	-0.75 <sup>h,m</sup>	≤ -0.48 <sup>m</sup>		
H .....	289.16	-1.45	-1.05	0.0	-1.18	-2.06
I .....	274.20	-0.23	+0.087	+0.30	-0.33	-0.72
D .....	270.52	-0.55	-0.109	+0.30	-0.61	-0.77
E .....	264.79	-0.31	+0.046	+0.43	-0.30	-0.46
F .....	257.39	-0.40 <sup>k</sup>	-0.45	+0.30	-0.83	-0.69
G .....	252.20	-0.89	-0.57	+0.30	(1.18)	-1.13
ao ....	226.02	...	-1.35 <sup>h</sup>	< -0.48 <sup>h</sup>		
aj ....	225.48	...	...	< -0.48 <sup>h</sup>		
ab ....	224.35	-1.0 <sup>h,k</sup>	-0.65 <sup>h</sup>	-0.125 <sup>h</sup>	-0.77 <sup>h</sup>	
az ....	223.20	-1.2 <sup>h,k</sup>	< -1.65 <sup>h</sup>	< -0.125 <sup>h</sup>	-1.27 <sup>h</sup>	
L .....	220.08	-0.56	-0.35	-0.18	-0.36	-0.77
K ....	219.12	-0.73	-0.48	0.0	-0.40	-0.63
ak ....	218.18	...	-1.05 <sup>n</sup>	< -0.18 <sup>n</sup>		
s.....	216.90	...	≤ -0.95 <sup>o</sup>	≤ -0.125 <sup>o</sup>		
al....	197.85	...	< -1.65 <sup>p</sup>			
am ...	193.72	...	< -1.65 <sup>p</sup>			

<sup>a</sup> Entries are  $\log R = \log(I_{\text{line}}/I_{211.3})$ .

<sup>b</sup> Keyed to Table 2A.

<sup>c</sup> Malinovsky & Heroux 1973; active solar disk.

<sup>d</sup> Behring et al. 1976.

<sup>e</sup> Dere 1978; flares.

<sup>f</sup> Dere 1982; active regions.

<sup>g</sup> Not included in spectral range.

<sup>h</sup> Present identification.

<sup>i</sup> Present in appreciable intensity.

<sup>j</sup> Blend with Ar XVI.

<sup>k</sup> Approximate measurement in published spectrum.

<sup>l</sup> Alternate identification Fe XI.

<sup>m</sup> Alternative identification Si IX.

<sup>n</sup> Alternative identification S XII.

<sup>o</sup> Alternative identifications Si VIII, Fe XIII.

<sup>p</sup> Unidentified but coincides with Fe XIV line; see text.

Two other published flare spectra are of some interest for the present study. Sandlin et al. (1976) (SBST) list an unidentified line of relatively low excitation class at 295.99 Å which is probably line *m*, and Widing (1978) lists an unidentified line of low excitation class at 355.86 Å which is probably line *v*. Positive identifications cannot be made however, at this time, in the absence of other Fe XIV lines for comparison.

Another line has been registered by several observers which is not due to Fe XIV but bears mentioning because it recurs in several lists as an unidentified or tentatively classified line: in the D78 list, the wavelength is given as  $242.07 \pm 0.03$  Å and is assigned to Fe XXI; in the list of SBST the wavelength is given as 242.07 Å; and the SERTS list includes what is apparently the same line at a wavelength of  $242.116 \pm 0.010$  Å. On the

TABLE 10  
SERTS—OBSERVED<sup>a</sup> RELATIVE LINE  
INTENSITIES<sup>b</sup>

(Å)	Line	(-)log R
447.34 .....	R	1.44
444.24 .....	N	1.91
429.54 .....	O	2.52
363.75 .....	ad <sup>c</sup>	1.96
358.67 .....	ae <sup>d</sup>	1.14
356.65 .....	C	1.69
353.83 .....	A	0.545
334.17 .....	B	0.201
290.71 .....	ag <sup>e</sup>	1.49
289.17 .....	H	1.14
274.21 .....	I	-0.00424
270.52 .....	D	0.319
264.78 .....	E	-0.00843
257.40 .....	F	0.737
252.20 .....	G	0.730
220.07 .....	L	0.605
219.12 .....	K	0.394

<sup>a</sup> Thomas & Neupert 1993.

<sup>b</sup>  $R = I_{\text{line}}/I_{211.3}$ .

<sup>c</sup> Ascribed to Mg VII; identified here as mainly Fe XIV.

<sup>d</sup> Blend with Fe XI; see text.

<sup>e</sup> Blend with Si IX; see text.

basis of laboratory measurements by Churilov et al. (1985) which give a wavelength of 242.100 Å, SK has proposed its classification as a line of Fe xv. It will be of interest to resolve the question of identification by a similar, extended analysis of the Fe xv spectrum.

### 3.2. Analysis of S082A Spectra

The NRL S082A slitless spectrograph flown on *Skylab* covered the wavelength range 170–630 Å with a maximum spectral resolution of approximately 0.1 Å and a spatial resolution of approximately 2"; it is described by Tousey et al. (1977) and D78. We searched the S082A archival spectra for the shorter wavelength lines suggested by SK to be Fe xiv lines, and measured their ratios relative to line *J* in three flare spectra observed on 1973 December 17 at 00:44:25 and 00:45:19 UT (discussed by Widing & Spicer 1980 and Widing & Cook 1987), and on 1974 January 21 at 23:27:36 (discussed by Hiei & Widing 1979 and Widing & Hiei 1984). The observed ratios are summarized in Table 11. In general they are considered to be accurate to within less than a factor of 2. The S082A instrument response falls off rapidly, however, below about 220 Å (Dere, private communication) so that lines at 193.75 Å and 197.78 Å are very weak with intensities near the background noise level; their measured ratios should therefore be considered as upper limits. In the case of a candidate line at 192.64 Å, also, it was not possible to obtain a measured ratio since it was masked by the Ca xvii line at 192.86 Å.

The S082A values are included as crosses in Figure 6, in a comparison with the predictions and with corresponding observations listed in Table 9. It is seen that the line features at 226.04 Å and 224.35 Å are confirmed as Fe xiv lines *ao* and *ab*. In the case of the line at 223.22 Å, the variation in observed intensities indicates that the Fe xiv transition *az* and a previously proposed Si ix line both contribute to the (wide) feature. Another transition *pp* at 223.26 Å, near the same wavelength, is found here to be more than a factor of 10 weaker than *az* (Fig. 2) and therefore negligible. From Figure 6 the observed line feature at 216.93 Å is a factor of about 25 stronger than the predicted intensity of Fe xiv transition *s*, indicating that it arises primarily from Si viii as previously classified. The line is very wide in the BCFD spectrum, however, so that transition *s* may be present as a minor blend.

Transition *aj*, expected near 225.48 Å, was not present in the S082A spectrum. This is consistent with the known instrumental sensitivity.

With respect to the shortest wavelength lines near 197.8 Å and 193.7 Å the situation remains unclear since present observations are not sufficient to arrive at a definite conclusion. It

seems likely, however, from the wavelength coincidences with the laboratory lines of RL, as well as the absence of other possibilities, that these are the Fe xiv transitions *al* and *am*, the latter identification being somewhat supported by Figure 6; further observations with greater sensitivity in this wavelength range would be desirable.

### 3.3. The Forbidden Transition *bn*

In most isoelectronic sequences all levels above those in the ground configuration can decay rapidly by one or more electric dipole transitions to lower levels, so that their populations are negligible compared to those in the ground configuration levels. The aluminum-like sequence is unique, however, in having one level, in the excited  $3s3p3d$  configuration, which cannot decay by an electric dipole transition; this is the  ${}^4F_{9/2}$  level which can decay only by a weak magnetic dipole transition to the neighboring  ${}^4F_{7/2}$  level. This means that when collisional excitation to this level from ground levels becomes appreciable, its population can build up to numbers comparable with those of the ground configuration levels; in other words, it is a metastable level. However, in contrast to usual metastable levels in the ground configuration which are collisionally closely coupled to ground levels even at low densities, because of small energy intervals, this high level is not collisionally coupled to the ground levels at low densities because of the large energy difference. The  ${}^4F_{9/2}$  level population will depend, in the coronal approximation, directly on the collision strengths  $\Omega({}^2P_{1/2,3/2} \rightarrow {}^4F_{9/2})$  and inversely on the magnetic dipole rate  $A(21 \rightarrow 18)$ . In the present calculation  $A(21 \rightarrow 18)$  is found to be  $12.4 \text{ s}^{-1}$ , and the collision strengths obtained (at 20 rydberg) are  $\Omega({}^2P_{1/2} \rightarrow {}^4F_{9/2}) = 4.7 \times 10^{-5}$ ,  $\Omega({}^2P_{3/2} \rightarrow {}^4F_{9/2}) = 0.021$ ; thus collisional excitation can become significant from the second level.

The calculated relative intensity variation of line *bn* [ $[3s3p3d]({}^4F_{9/2} \rightarrow {}^4F_{7/2})$ ] with density is shown in Figure 3. As expected, the relative population of the  ${}^4F_{9/2}$  level increases with electron density and reaches a pronounced maximum at  $N_e = 10^{10} \text{ cm}^{-3}$ , where the intensity of line *bn* is a factor of only fifty less than that of the observed intercombination line *P*. Below this density, the *bn* line excitation process is in the coronal regime; above this density the excitation process is in the Boltzmann regime and the population of the  ${}^4F_{9/2}$  level, relative to the populations of the upper levels of the resonance lines (which are still in their coronal regimes), drops again. As seen in Figure 3, its relative intensity decrease then mirrors that of the coronal green line *M*.

The peak of relative intensity is thus reached at the critical density of line *bn* which marks the boundary between coronal and Boltzmann conditions (cf. Sobelman, Vainshtein, & Yukov

TABLE 11  
OBSERVED S082A LINE RATIOS<sup>a</sup>

SOLAR FLARE	WAVELENGTH (Å)					
	193.75	197.78	216.93	223.22	224.35	226.04
1973 Dec 17 00:44:25 UT .....	$\leq -0.936$	...	-0.708	-0.955	-1.04	
1973 Dec 17 00:45:19 UT .....	...	...	-0.611	-0.932	...	-1.40
1974 Jan 21 23:27:36 UT .....	$\leq -0.662$	$\leq -1.08$	-0.767	-0.812	-0.815	-0.827

<sup>a</sup> Entries are  $\log R \equiv \log(I_\lambda/I_{211.3})$ .

1981). We note that this is in marked contrast to a conventional interpretation of "critical density" as the density at which forbidden lines from metastable levels become "quenched." The difference is essentially due to the fact that normally a metastable level lies (well) below the upper levels of allowed resonance and subordinate lines, whereas here the metastable level lies above such levels.

It is likely also that in time-dependent situations the temporal variation of such a line will be qualitatively different from that of allowed lines, intercombination lines, or usual forbidden lines, a feature which may be potentially useful for diagnostic purposes.

The question of observability of the line is then relevant. According to the level energies calculated by FL and KH the wavelength would be respectively 1.282  $\mu\text{m}$  or 1.218  $\mu\text{m}$ , in the near-infrared; the difference between these two values is a measure of the kind of accuracy obtainable with respect to fine-structure splittings in such detailed calculations. At the same time, observational material in this wavelength range is not extensive. We have here established that the line reaches maximum relative intensity at  $10^{10} \text{ cm}^{-3}$ , a density existing in the solar transition region between chromosphere and corona. Eclipse observations might therefore be capable of detecting the line. Kastner (1993) notes that a line of unknown origin is present at 1.266  $\mu\text{m}$  in the eclipse spectrum recorded by Olson et al. (1971), which could conceivably be the line *bn*. Another interesting possibility for observing the line may exist in the fact that Fe XIV emission in the coronal green line has been observed in some expanding novae envelopes, e.g., by Wallerstein & Garnavich (1986) in RS Oph. As expansion proceeds

density decreases, passing through densities of the order of  $10^{10} \text{ cm}^{-3}$  according to observed coronal ion lines (cf. Greenhouse et al. 1990). Observations of novae in the near-infrared *J* band around 1.2  $\mu\text{m}$  with sufficient sensitivity to detect this line might therefore be worthwhile.

#### 4. SUMMARY

The results of this analysis for the presence of the weaker Fe XIV lines in solar spectra are summarized in Table 12, which groups them into three categories: (a) confirmed as present by quantitative agreement between observations and predictions for both wavelengths and intensities, (b) present with a high probability on the basis of coincidence between observed and predicted wavelengths alone, (c) possibly present, with some doubt introduced, e.g., by low signal-to-noise level. Of the 10 transitions proposed by SK to account for lines in the BCFD spectrum, six are verified and three remain probable. The S082A-observed line at 216.93 Å is shown to be inconsistent in intensity with the suggested Fe XIV transition *s*, so that a present classification of Si VIII is probably correct (but should in principle be verified by a similar independent analysis of the Si VIII spectrum; the observed line is wide, also). With respect to the shorter wavelength solar lines at 197.78 Å, 193.75 Å, and 192.64 Å, present observational material is not adequate to decide the case due to decreased instrumental sensitivities below about 200 Å. However, we include them in the "probable" class on the basis of striking wavelength agreement and lack of other possible identifications.

In addition to the transitions discussed by SK and investigated here, the resonance line *C* (356.64 Å) has been verified to

TABLE 12  
CONFIRMED,<sup>a</sup> PROBABLE,<sup>b</sup> AND POSSIBLE<sup>c</sup> SOLAR OBSERVATIONS OF THE WEAKER Fe XIV LINES

Line	(Å)	BCFD <sup>d</sup>	SBST <sup>e</sup>	W78 <sup>f</sup>	D78 <sup>g</sup>	D82 <sup>h</sup>	SERTS <sup>i</sup>	S082A <sup>j</sup>
<i>P</i> .....	484.60							Y <sup>k</sup>
<i>Q</i> .....	467.40			P	Y <sup>l</sup>			Y <sup>k</sup>
<i>R</i> .....	447.36			Y	Y <sup>l</sup>			Y <sup>k</sup>
<i>N</i> .....	444.25							Y <sup>k</sup>
<i>O</i> .....	429.54						Y	Y <sup>k</sup>
<i>ad</i> .....	363.75						Y <sup>l</sup>	
<i>ae</i> .....	358.67	Y <sup>l</sup>					Y <sup>l</sup>	
<i>C</i> .....	356.64						Y	
<i>v</i> .....	355.86						P <sup>l</sup>	
<i>m</i> .....	295.99			P <sup>l</sup>				
<i>ag</i> .....	290.7	Y <sup>l</sup>					Y <sup>l</sup>	
<i>ao</i> .....	226.04	Y <sup>l</sup>			Y <sup>l</sup>			Y <sup>l</sup>
<i>aj</i> .....	225.48				?			
<i>ab</i> .....	224.35	Y <sup>l</sup>			Y <sup>l</sup>	Y <sup>l</sup>		Y <sup>l</sup>
<i>az</i> .....	223.22	Y <sup>l</sup>			Y <sup>l</sup>	Y <sup>l</sup>		Y <sup>l</sup>
<i>ak</i> .....	218.18	Y <sup>l</sup>			Y <sup>l</sup>			
<i>s</i> .....	216.93	m			m			m
<i>i</i> .....	212.35	P <sup>l</sup>						
<i>al</i> .....	197.85	P						?
<i>am</i> .....	193.75	P						?

<sup>a</sup> Entry is Y(es).

<sup>b</sup> Entry is P(robable).

<sup>c</sup> Entry is a question mark.

<sup>d</sup> Behring et al. 1976.

<sup>e</sup> Sandlin et al. 1976.

<sup>f</sup> Widing 1978.

<sup>g</sup> Dere 1978.

<sup>h</sup> Dere 1982.

<sup>i</sup> Thomas & Neupert 1993.

<sup>j</sup> Present S082A-measured intensities.

<sup>k</sup> Previously confirmed; Keenan et al. 1991.

<sup>l</sup> Present identification.

<sup>m</sup> Negative confirmation; observed line feature not due to Fe XIV.

be present (only) in the SERTS spectrum, and the transition *ad* (363.75) has been shown to be present (only) in the same spectrum. The line *i* (212.35 Å) has been identified in the BCFD list and the lines *m* (295.99 Å) and *v* (355.86 Å) have been identified in the spectral lists of Sandlin et al. (1976) and Widing (1978), though these three lines still need verification on the basis of observed relative intensities. Also, we have found the intercombination lines *Q* and *R* and the transitions *ab* and *az* in the list of unidentified lines given for active regions by D82.

The solar line feature observed in the vicinity of 290.7 Å requires some comment. The BCFD-measured wavelength is  $290.710 \pm 0.010$  Å, while the wavelength given by RL for the Fe XIV transition *ag* is  $290.75 \pm 0.02$  Å. The SERTS-measured wavelength of the solar feature, on the other hand, is  $290.693 \pm 0.009$  Å. According to the level values given by Edlen (1985) the transition  $2s2p^3(^3P_1) \rightarrow 2s^22p^2(^3P_0)$  in Si IX would occur at 290.69 Å, so that identification with the Si IX line might seem reasonable on the basis of wavelengths.

- Arnaud, M., & Rothenflug, R. 1985, A&AS, 60, 425  
 Behring, W. E., Cohen, L., Feldman, U., & Doschek, G. A. 1976, ApJ, 203, 521 (BCFD)  
 Bhatia, A. K., & Kastner, S. O. 1980, Sol. Phys., 65, 181  
 ———. 1989, ApJS, 71, 665  
 ———. 1993, J. Quant. Spectrosc. Rad. Transfer, 49, 609  
 Blaha, M. 1971, Sol. Phys., 17, 99 (MB)  
 Churilov, S. S., Kononov, E. Y., Ryabtsov, A. M., & Zayakin, Y. F. 1985, Phys. Scripta, 32, 501  
 Dere, K. P. 1978, ApJ, 221, 1062 (D78)  
 ———. 1982, Sol. Phys., 77, 77 (D82)  
 Dere, K. P., Mason, H. E., Widing, K. G., & Bhatia, A. K. 1979, ApJS, 40, 341  
 Dufton, P. L., & Kingston, A. E. 1991, Phys. Scripta, 43, 386 (DK)  
 Edlen, B. 1985, Phys. Scripta, 31, 345  
 Eissner, W., Jones, M., & Nussbaumer, H. 1972, Comput. Phys. Comm., 8, 270  
 Eissner, W., & Seaton, M. J. 1972, J. Phys., B, 5, 2187  
 Farrag, A., Luc-Koenig, & Sinzelle, J. 1982, Atom. Data Nucl. Data Tables, 27, 539  
 Fawcett, B. 1983, Atom. Data Nucl. Data Tables, 28, 557  
 Froese Fischer, C., & Liu, B. 1986, Atom. Data Nucl. Data Tables, 34, 261 (FL)  
 Greenhouse, M. A., Grasdalen, G. L., Woodward, C. E., Benson, J., Gehr, R. D., Rosenthal, E., & Skrutskie, M. F. 1990, ApJ, 352, 307  
 Hiei, E., & Widing, K. G. 1979, Sol. Phys., 61, 407  
 Huang, K.-N. 1986, Atom. Data Nucl. Data Tables, 34, 1 (KH)  
 Kastner, S. O. 1985, J. Quant. Spectrosc. Rad. Transfer, 34, 21  
 ———. 1991, Sol. Phys., 135, 343 (SK)  
 ———. 1993, Sol. Phys., 143, 197

However, we have shown here (Fig. 5) that on the basis of observed intensity the solar feature, in active regions at least, is certainly due to the Fe XIV transition *ag*. It is probable therefore that the Si IX transition and the Fe XIV transition *ag* coincide in wavelength at 290.69 Å, which would put the Fe XIV level 20 [ $3p^3(^2P_{3/2})$ ] at about  $645480 \text{ cm}^{-1}$  rather than the RL value of  $645416 \text{ cm}^{-1}$ .

Finally, we have stressed the unique nature of a forbidden line emitted from a very high level in the Fe XIV system. In future work authors A. K. B. and S. O. K. plan to investigate this type of line more extensively.

We wish to thank D. A. Bowden for reducing the S082A data, and E. S. C. acknowledges financial support from the SERC.

This work was supported by NASA-RTOP grant 188-38-53-14 and NATO travel grant 0469/87.

## REFERENCES

- Keenan, F. P., Dufton, P. L., Boylan, M. B., Kingston, A. E., & Widing, K. G. 1991a, ApJ, 373, 695  
 Keenan, F. P., Dufton, P. L., Conlon, E. S., Boylan, M. B., Kingston, A. E., & Widing, K. G. 1991b, ApJ, 379, 406  
 Levashov, V. E., Ryabtsev, A. N., & Churilov, S. S. 1990, Opt. Spectrosc., 69, 20  
 Malinovsky, M., & Heroux, L. 1973, ApJ, 181, 1009 (MH)  
 Mason, H. E. 1975, MNRAS, 170, 651  
 Neupert, W. M. 1986, Proc. Soc. Optical Eng., 689, 224  
 Olsen, K. H., Anderson, C. R., & Stewart, J. N. 1971, Solar Phys., 21, 360  
 Petrini, D. 1970, A&A, 9, 392  
 Redfors, A., & Litzen, U. 1989, J. Opt. Soc. Am. B, 6, 1447 (RL)  
 Sandlin, G. D., Brueckner, G. E., Scherrer, V. E., & Tousey, R. 1976, ApJ, 205, L47 (SBST)  
 Saraph, H. E. 1972, Comput. Phys. Comm., 3, 256  
 Shirai, T., Funatake, Y., Mori, K., Sugar, J., Wiese, W. L., & Nakai, Y. 1990, J. Phys. Chem. Ref. Data, 19, 127  
 Sobelman, I. I., Vainshtein, L. A., & Yukov, E. A. 1981, Excitation of Atoms and Broadening of Spectral Lines (Berlin: Springer-Verlag)  
 Thomas, R. J., & Neupert, W. M. 1993, ApJ, submitted  
 Tousey, R., Bartoe, J.-D. F., Brueckner, G. E., & Purcell, J. D. 1977, Appl. Optics, 16, 870  
 Trabert, E., Hutton, R., & Martinson, I. 1987, MNRAS, 227, 27P  
 Wallerstein, G., & Garnavich, P. M. 1986, PASP, 98, 875  
 Widing, K. G. 1978, ApJ, 222, 735  
 Widing, K. G., & Cook, J. W. 1987, ApJ, 320, 913  
 Widing, K. G., & Hiei, E. 1984, ApJ, 281, 426  
 Widing, K. G., & Spicer, D. S. 1980, ApJ, 242, 1243